

Spin dynamics in lightly doped $\text{La}_{2-x}\text{Sr}_x\text{CuO}_4$: Relaxation function within the $t - J$ model

Igor A. Larionov*

Magnetic Radiospectroscopy Laboratory, Department of Physics, Kazan State University, 420008 Kazan, Russia

The relaxation function theory of doped two-dimensional $S = 1/2$ Heisenberg antiferromagnetic (AF) system in the paramagnetic state is presented taking into account the hole subsystem as well as both the electron and AF correlations. The expression for fourth frequency moment of relaxation shape function is derived within the $t - J$ model. The presentation obeys rotational symmetry of the spin correlation functions and is valid for all wave vectors through the Brillouin zone. The spin diffusion contribution to relaxation rates is evaluated and is shown to play a significant role in carrier free and doped antiferromagnet in agreement with exact diagonalization calculations. At low temperatures the main contribution to the nuclear spin-lattice relaxation rate, $^{63}(1/T_1)$, of plane ^{63}Cu arises from the AF fluctuations, and $^{17}(1/T_1)$, of plane ^{17}O , has the contributions from the wavevectors in the vicinity of (π, π) and small $q \sim 0$. It is shown that the theory is able to explain the main features of experimental data on temperature and doping dependence of $^{63}(1/T_1)$ in the paramagnetic state of both carrier free La_2CuO_4 and doped $\text{La}_{2-x}\text{Sr}_x\text{CuO}_4$ compounds.

PACS numbers: 74.72.Dn, 74.25.Ha, 75.40.Gb, 71.27.+a

I. INTRODUCTION

The spin dynamics in doped two-dimensional $S = 1/2$ Heisenberg antiferromagnetic (2DHAF) systems remains the one of the intriguing problems of condensed matter in connection with physics of layered copper High Temperature Superconductors (HTSC).¹ The effect of doped holes in two-dimensional (2D) antiferromagnetic (AF) background was studied in many papers.² The Hohenberg-Mermin-Wagner theorem states the absence of long range order in low-dimensional isotropic Heisenberg systems at any finite temperature due to fluctuations, making the order short-ranged. The temperature dependence of correlation length in two-dimensional Heisenberg model was first described by Chakravarty, Halperin and Nelson (CHN) by a quantum nonlinear σ model³ in accord with neutron scattering (NS) experiments⁴ in carrier free La_2CuO_4 . A significant advance was achieved in understanding the 2D Heisenberg systems at low temperatures due to the improved further results of CHN in the renormalized classical regime.^{5,6} Since then the temperature dependence of correlation length has been studied, e.g., by isotropic wave theory⁷ and by quantum consideration of skyrmions.⁸

Nuclear Quadrupole Resonance (NQR) and Nuclear Magnetic Resonance (NMR) methods are very powerful in studying the low energy excitations of HTSC.¹ Chakravarty and Orbach⁹ developed a theory of magnetic relaxation phenomena in 2DHAF based on the quantum

nonlinear σ model of CHN in the critical region of fluctuations. However, they considered only the contribution that arises from the wave vectors in the vicinity of AF wave vector (π, π) . Despite the fact that contribution from the wave vectors $\mathbf{q} \sim 0$ does not dominate in the plane copper spin-lattice relaxation rate at low temperatures and was not accounted in the analysis,¹⁰ the contribution from spin diffusion plays an important role in HTSC, especially in the plane oxygen relaxation rate as measured by NMR, since the AF fluctuating contribution is filtered out by the oxygen formfactor.

The Nearly Antiferromagnetic Fermi Liquid (NAFL) model of Millis, Monien and Pines¹¹ reconciled the puzzling observation of non-Korringa temperature dependence of the copper nuclear spin-lattice relaxation rate and Korringa temperature dependence of the oxygen and yttrium nuclear spin-lattice relaxation rates in optimally doped $\text{YBa}_2\text{Cu}_3\text{O}_7$ by postulating both the localized Cu^{2+} magnetic moments and free oxygen holes. The NAFL model gave the relation between the AF correlation length and the relaxation rates and was applied in a wide temperature and doping range.¹² However, this theory has some disadvantages, connected mainly with the phenomenological character of the NAFL description, since the temperature and doping dependence of correlation length was postulated or, at best, taken from a comparison with experiment.

As a consequence, it is tempting to consider the 2DHAF systems doped by charge carriers microscopically and the difficulties rise on. The numerically exact methods study the relatively small clusters and in addition, these methods are hardly applicable if we need to obtain the dynamic quantities. In the absence of exact solution it is necessary to find a reliable approach that will describe the physical quantities with convincing accuracy. This is intriguing especially since the observation of drastic change of various physical quantities with doping and emergence of "stripe" physics in doped HTSC and related compounds.

The $t - J$ model became very popular since it was pointed by Anderson¹³ as a perspective model to describe the electronic properties of layered HTSC cuprates. The present theory is developed for paramagnetic state using a Mori-Zwanzig projection operator procedure,^{14,15} with a three-pole approximation for the relaxation function.¹⁶ The merits of the theory were demonstrated¹⁶ by comparison with experiments in antiferromagnets in a wide temperature range down to temperatures close to Neel temperature T_N . The advantage of the present formulation is that it allows to take into account not only the AF correlation effects in relaxation rates, but also the contribution from spin diffusion. The presentation of the $t - J$ model in terms of Hubbard operators is known to obey the rotational symmetry of the spin correlation functions and automatically guarantees the exclusion of

double occupancy. The form of static susceptibility will be used from microscopic theory¹⁷ as obtained beyond the Random Phase Approximation (RPA) and naturally takes into account the contribution from the hole subsystem. The dynamic structure factor is a quantity directly measured in various experiments, e.g., by magnetic neutron scattering. The advantages of expressing the dynamic structure factor in terms of relaxation function were shown by Mori and Kawasaki.¹⁸ Until present the Mori-Zwanzig projection operator procedure was applied in connection with HTSC only to carrier free 2D $S = 1/2$ AF system¹⁹ with a three-pole approximation for the relaxation function¹⁶ and the correlation length was used from the results of CHN.³ It should be emphasized that the method developed in the present work for calculations of dynamic structure factor and nuclear spin-lattice relaxation rates is similar, however, the approach is different from the calculations with the approximations for dynamic spin susceptibilities.^{20,1,11,17,21,22}

The paper is organized as follows. In Sec. II, the basic relations are presented for the relaxation function with a three pole approximation in a continued fraction representation of the Laplace transform and the static spin susceptibility. Sec. III shows the evaluation of the second and the fourth frequency moments of relaxation shape function within the $t - J$ model. Sec. IV presents the results of calculations, comparison with experiment, other theories and discussion. Sec. V is the Conclusion.

II. BASIC RELATIONS

We employ the $t - J$ Hamiltonian written in terms of the Hubbard operators:

$$H_{t-J} = H_t + H_J = \sum_{i,j,\sigma} t_{ij} X_i^{\sigma 0} X_j^{0\sigma} + J \sum_{i>j} \left(\mathbf{S}_i \mathbf{S}_j - \frac{1}{4} n_i n_j \right). \quad (1)$$

Here, \mathbf{S}_i are spin-1/2 operators at the lattice sites i , and $X_i^{\sigma 0}$ are the Hubbard operators that create an electron with spin σ at site i . The hopping integral t_{ij} describes the motion of electrons causing a change in their spins. In this paper, $t_{ij} = t$ refers to hopping between nearest neighbors and J is the nearest-neighbor antiferromagnetic (AF) coupling constant. The spin and density operators are defined as follows:

$$S_i^\sigma = X_i^{\sigma \tilde{\sigma}}, \quad S_i^z = \frac{1}{2} \sum_{\sigma} \sigma X_i^{\sigma \sigma}, \quad (2)$$

$$n_i = \sum_{\sigma} X_i^{\sigma \sigma}, \quad (\sigma = -\tilde{\sigma}), \quad (3)$$

with the standard normalization $X_i^{00} + X_i^{++} + X_i^{--} = 1$. Without loss of generality, we measure all energies from the "center of gravity" of the band.

A. Mori-Zwanzig projection operator procedure and a three pole approximation for the dynamic relaxation function

In the present formulation we will follow Mori.¹⁴ The time evolution of a dynamical variable $S_{\mathbf{k}}^z(\tau)$, say, is given by

$$\dot{S}_{\mathbf{k}}^z(\tau) \equiv \frac{dS_{\mathbf{k}}^z(\tau)}{d\tau} = iL S_{\mathbf{k}}^z(\tau). \quad (4)$$

In general, L is the Liouville operator, and in our, quantal case, $iL S_{\mathbf{k}}^z(\tau)$ is the corresponding commutator with the Hamiltonian (1). The projection of the vector $S_{\mathbf{k}}^z(\tau)$ onto the $S_{\mathbf{k}}^z \equiv S_{\mathbf{k}}^z(\tau = 0)$ axis is given by

$$\mathcal{P}_0 S_{\mathbf{k}}^z(\tau) = R(\mathbf{k}, \tau) \cdot S_{\mathbf{k}}^z, \quad (5)$$

and defines the linear projection Hermitian operator \mathcal{P}_0 . One may separate $S_{\mathbf{k}}^z(\tau)$ into the projective and vertical components with respect to the $S_{\mathbf{k}}^z$ axis:

$$S_{\mathbf{k}}^z(\tau) = R(\mathbf{k}, \tau) \cdot S_{\mathbf{k}}^z + (1 - \mathcal{P}_0) S_{\mathbf{k}}^z(\tau), \quad (6)$$

where

$$R(\mathbf{k}, \tau) \equiv (S_{\mathbf{k}}^z(\tau), (S_{-\mathbf{k}}^z)^*) \cdot (S_{\mathbf{k}}^z, (S_{-\mathbf{k}}^z)^*)^{-1}, \quad (7)$$

is the relaxation function in the inner-product bracket notation:

$$(S_{\mathbf{k}}^z(\tau), (S_{-\mathbf{k}}^z)^*) \equiv k_B T \int_0^{1/k_B T} d\varrho \times \langle \exp(\varrho H) S_{\mathbf{k}}^z(\tau) \exp(-\varrho H) (S_{-\mathbf{k}}^z)^* \rangle, \quad (8)$$

where the angular brackets denote the thermal average.

For future evaluations, it is convenient to introduce a set of quantities $f_0(\tau), f_1(\tau), \dots, f_j(\tau), \dots$ defined by equations

$$f_j(\tau) \equiv \exp(iL_j \tau) f_j \equiv \exp(iL_j \tau) iL_j f_{j-1}, \quad (j \geq 1), \quad (9)$$

where $f_0(\tau) \equiv S_{\mathbf{k}}^z(\tau)$, $L_j \equiv (1 - \mathcal{P}_{j-1})L_{j-1}$, ($L_0 = L$), and

$$\Delta_j^2 \equiv (f_j, f_j^*) \cdot (f_{j-1}, f_{j-1}^*)^{-1}. \quad (10)$$

The set $\{f_j\}$ forms an orthogonal set. The larger number of f_j is used, the finer description of $S_{\mathbf{k}}^z(\tau)$ is obtained. The last quantity from this set f_n , affected by evolution operator $\exp(iL_n \tau)$, resulting in $f_n(\tau)$, was called the "n-th order random force",¹⁴ acting on the variable $S_{\mathbf{k}}^z(\tau)$ and is responsible for fluctuation from its average motion.

In terms of Laplace transform of the relaxation function, $R^L(\mathbf{k}, \tau)$, one may construct a continued fraction representation for $R(\mathbf{k}, s)$:

$$R^L(\mathbf{k}, s) = \int_0^\infty d\tau e^{s\tau} R(\mathbf{k}, \tau) = 1 / \{s + \Delta_{1\mathbf{k}}^2 / [s + \Delta_{2\mathbf{k}}^2 / (s + \Delta_{3\mathbf{k}}^2 / \dots)]\}, \quad (11)$$

where $\Delta_{j\mathbf{k}}^2$ are related to the frequency moments

$$\langle \omega_{\mathbf{k}}^n \rangle = \int_{-\infty}^\infty d\omega \omega^n F(\mathbf{k}, \omega) = \frac{1}{i^n} \left[\frac{d^n R(\mathbf{k}, \tau)}{d\tau^n} \right]_{\tau=0} \quad (12)$$

of the relaxation shape function

$$F(\mathbf{k}, \omega) = \frac{1}{\pi} \text{Re}[R^L(\mathbf{k}, i\omega)] \\ = \frac{1}{2\pi} \int_{-\infty}^{\infty} d\tau e^{-i\omega\tau} R(\mathbf{k}, \tau), \quad (13)$$

as

$$\Delta_{1\mathbf{k}}^2 = \langle \omega_{\mathbf{k}}^2 \rangle, \quad \Delta_{2\mathbf{k}}^2 = \frac{\langle \omega_{\mathbf{k}}^4 \rangle}{\langle \omega_{\mathbf{k}}^2 \rangle} - \langle \omega_{\mathbf{k}}^2 \rangle. \quad (14)$$

Lovesey and Meserve¹⁶ truncated the relaxation function (11) to third order. They argued that since the \mathbf{k} dependence of $\Delta_{2\mathbf{k}}$ is much weaker than that of $\Delta_{1\mathbf{k}}$, and using the analytical results²³ for the sixth frequency moment $\langle \omega_{\mathbf{k}}^6 \rangle$, the approximation of $\Delta_{3\mathbf{k}}$ by a constant is a good approximation. Thus, they suggested a three pole approximation for relaxation function,

$$R(\mathbf{k}, s) = 1/\{s + \Delta_{1\mathbf{k}}^2/[s + \Delta_{2\mathbf{k}}^2/(s + 1/\tau_{\mathbf{k}})]\}, \quad (15)$$

with a cutoff characteristic time

$$\tau_{\mathbf{k}} = \left(\frac{2}{\pi \Delta_{2\mathbf{k}}^2} \right)^{1/2}. \quad (16)$$

For $F(\mathbf{k}, \omega)$ this is equivalent to

$$F(\mathbf{k}, \omega) = \frac{\tau_{\mathbf{k}} \Delta_{1\mathbf{k}}^2 \Delta_{2\mathbf{k}}^2 / \pi}{[\omega \tau_{\mathbf{k}} (\omega^2 - \Delta_{1\mathbf{k}}^2 - \Delta_{2\mathbf{k}}^2)]^2 + (\omega^2 - \Delta_{1\mathbf{k}}^2)^2}. \quad (17)$$

Here one should note that $F(\mathbf{k}, \omega)$ is real, normalized to unity $\int_{-\infty}^{\infty} d\omega F(\mathbf{k}, \omega) = 1$ and even in both \mathbf{k} and ω .

The dynamic structure factor $S(\mathbf{k}, \omega)$ is related to the relaxation shape function $F(\mathbf{k}, \omega)$ through the fluctuation-dissipation theorem

$$S(\mathbf{k}, \omega) = \frac{2\pi\omega\chi(\mathbf{k})}{1 - \exp(-\omega/k_B T)} F(\mathbf{k}, \omega). \quad (18)$$

The only undefined quantity in the present formulation is the static spin susceptibility $\chi(\mathbf{k})$ in (18). Until present this method was used¹⁶ to describe the paramagnetic state properties of (anti)ferromagnets with the form of static susceptibility, which was justified only at high temperatures (see also Refs. 24 and 19). In the present work we will employ the microscopic formula for static spin susceptibility¹⁷ that is shown to work in the overall temperature range and properly takes into account the hole subsystem.

B. Static spin susceptibility

From Ref. 17, the expression for static spin susceptibility $\chi(\mathbf{k})$ is straightforward,

$$\chi(\mathbf{k}) = \frac{4|c_1|}{Jg_-(g_+ + \gamma_{\mathbf{k}})}, \quad (19)$$

and its structure is the same as in the isotropic spin-wave theory.⁷ The meaning of g_+ is clear: it is related to the correlation length ξ via the expression

$$\frac{\xi}{a} = \frac{1}{2\sqrt{g_+ - 1}}, \quad (20)$$

where a is a lattice unit. For carrier free AF system the relation (20) was obtained from the exponential decay of the spin-spin correlation function at large separations, whereas at finite doping the same expression was derived from the expansion of $\chi(\mathbf{k})$ taken around the AF wave vector \mathbf{Q} , however, taking now into account the contribution from the hole subsystem.¹⁷

$$c_1 = \frac{1}{z} \sum_{\rho} \langle S_i^z S_{i+\rho}^z \rangle, \quad c_2 = \frac{1}{z^2 - z} \sum_{\rho \neq \rho'} \langle S_i^z S_{i+\rho-\rho'}^z \rangle, \quad (21)$$

are the nearest and next-nearest neighbor spin correlation functions, respectively, the index ρ runs over nearest neighbors, and

$$\gamma_{\mathbf{k}} = \frac{1}{z} \sum_{\rho} \exp(i\mathbf{k}\rho) = \frac{1}{2} (\cos k_x a + \cos k_y a), \quad (22)$$

$g_- = 4\alpha z|c_1|$, $z = 4$ is the number of nearest neighbors for square lattice. The parameters α and β were introduced in the decoupling procedures for the higher-order Green's functions.²⁵ The parameter α preserves the important property that spin operators obey the relation $\langle \mathbf{S}_i^2 \rangle = 3/4$ which should hold at all temperatures. The numerical values for the temperature dependence of ξ were determined in carrier free La_2CuO_4 using $J = 0.12$ eV and treating β as the only adjustable parameter.¹⁷ The best fit to experimental data, which were deduced from NS,⁴ was obtained with $\beta = 2.5$. This value will be kept fixed in the present calculations. The original self-consistent theory of Kondo and Yamaji (KY)²⁵ with $\alpha = \beta = 1.705$ fails in explanation of the absolute values of ξ . Since β enters in the combination βc_2 , the increase of the values of next-nearest correlations causes the extension of short-range AF order and hence the enhancement of ξ together with the spin stiffness constant ρ_S .¹⁷ In $T \rightarrow 0$ limit, for both the carrier free and doped case, c_2 and g_- are related as,

$$g_- = \frac{4}{3} (1 + 12c_2\beta). \quad (23)$$

The reliability of the theory has been demonstrated by comparing the numerical values for c_1 , c_2 and $\chi_S \equiv \chi(\mathbf{k} = 0)$ with Monte Carlo, Exact Diagonalization calculations and other theories.¹⁷

In the present calculations for small doping δ we will use the expression for doping and temperature dependence of ξ , given by,¹⁷

$$\frac{\xi}{a} = \frac{J\sqrt{g_-}}{k_B T} \exp(2\pi\rho_S/k_B T). \quad (24)$$

As discussed in Ref. 17, ξ diverges at $T = 0$ even in doped samples and this disagrees with experiment. This disagreement appears, probably, due to the overestimation of the role of AF correlations at low temperatures in the KY decoupling procedure. To mimic the low temperature behavior of the correlation length we will use the expression, as in Refs. 21, 22, resulting in *effective* correlation length ξ_{eff} , given by,

$$\xi_{eff}^{-1} = \xi_0^{-1} + \xi^{-1}. \quad (25)$$

Thus, the theory is able to explain the temperature and doping dependence of correlation length. The expression (25) is different from Keimer *et al.*²⁶ empirical equation, where ξ is given by the Hasenfratz-Niedermayer formula⁵ and hence, there is no influence of the hole subsystem on ξ . In contrast, in the present theory, ξ is affected by doped holes. Thus from now on we replace ξ by ξ_{eff} .

C. Excitation spectrum

The band evolution with doping remains the controversial topic. The usual parameter set in the $t - J$ model is $t = J/0.3$.² The electronic and AF spin-spin correlation functions reduce the hoppings²⁷ resulting in *effective* values. In the early proposal of $t - J$ model by Anderson^{13,28} for description of properties of layered copper HTSC compounds the phenomenological relation was settled for the band width $\sim \delta t$. Following the idea of Zhang and Rice²⁹ about copper-oxygen singlets formation it was shown by Eremin *et al.*,³⁰ that it is possible to describe correctly the elementary excitations spectrum in cuprates. This singlet correlated band is analogous to upper Hubbard band with essential distinction - the subband splitting is much smaller compared to Hubbard model. Therefore it is possible to apply Hubbard formalism without strict restriction on t and J values in $t - J$ model.³⁰ Taking into account the AF spin-spin correlations selfconsistently, resulting in *effective* hoppings, it was shown that the band width varies linearly with doping in a wide range from lightly doped to optimally doped compounds.²¹ To avoid confusion from approximations the simple expression for *effective* hopping

$$t_{eff} = \delta J/0.3, \quad (26)$$

will be employed in the following evaluations to match the insulator - metal transition. At high hole concentrations ($\delta \sim 1$), where the correlation effects are negligible, Eq. (26) gives, as it should, the value of band width for the noninteracting case.

Thus, $E_{\mathbf{k}}$ is given by

$$E_{\mathbf{k}} = 2t_{eff}(\cos k_x a + \cos k_y a). \quad (27)$$

This expression resembles well also the values of singlet-correlated bandwidth ≈ 0.4 eV (see Ref. 30) in optimally doped ($\delta \approx 0.15$ per Cu site) layered copper HTSC as obtained from Angle Resolved Photoemission Electron Spectroscopy (ARPES).³¹

III. EVALUATION OF EXPRESSIONS FOR FREQUENCY MOMENTS

We now describe the procedure used to calculate the second $\langle \omega_{\mathbf{k}}^2 \rangle$ and fourth $\langle \omega_{\mathbf{k}}^4 \rangle$ frequency moments of $F(\mathbf{k}, \omega)$, by calculating directly the corresponding commutators in

$$\langle \omega_{\mathbf{k}}^2 \rangle = i \langle [\dot{S}_{\mathbf{k}}^z, S_{-\mathbf{k}}^z] \rangle / \chi(\mathbf{k}), \quad (28)$$

and

$$\langle \omega_{\mathbf{k}}^4 \rangle = i \langle [\ddot{S}_{\mathbf{k}}^z, \dot{S}_{-\mathbf{k}}^z] \rangle / \chi(\mathbf{k}). \quad (29)$$

The main effort necessary here is to obtain the expression for $\langle \omega_{\mathbf{k}}^4 \rangle$. In this Section we will start with evaluation of commutators and calculation of the thermodynamic averages, then introduce the decoupling procedures and, finally, present the result for $\langle \omega_{\mathbf{k}}^4 \rangle$. The procedure will be tested by comparison of our expression for spin part with the existing result.¹⁶ The $X_i^{0\sigma}$ and $X_i^{\sigma 0}$ operators are fermions and obey the anticommutation relations, whereas the S_i^σ and $X_i^{\sigma\sigma}$ are bosonic-like and obey the commutation relations. The terms with the operators of different type are assumed to satisfy the commutation relations. The commutators with the products of operators were decomposed on terms that contain commutators and(or) anticommutators depending on the type of operators.

A. Evaluation of commutators

In order to calculate the second $\langle \omega_{\mathbf{k}}^2 \rangle$ and the fourth $\langle \omega_{\mathbf{k}}^4 \rangle$ frequency moments we first evaluate the commutators

$$[S_m^z, H_J] = \frac{1}{4} \sum_{j,\sigma} J_{mj} \sigma (S_m^\sigma S_j^{\tilde{\sigma}} - S_j^\sigma S_m^{\tilde{\sigma}}), \quad (30)$$

and

$$[S_m^z, H_t] = \frac{1}{2} \sum_{j,\sigma} t_{mj} \sigma (X_m^{\sigma 0} X_j^{0\sigma} - X_j^{\sigma 0} X_m^{0\sigma}). \quad (31)$$

The commutator of expression given by Eq. (31) with the hopping term H_t in (1) is

$$[[S_m^z, H_t], H_t] = \sum_{i,l,\sigma} t_{lm} \sigma \left\{ \frac{1}{2} t_{il} \left[X_m^{\sigma 0} X_l^{\tilde{\sigma} 0} X_i^{0\tilde{\sigma}} + X_m^{\sigma 0} (X_l^{00} + X_l^{\sigma\sigma}) X_i^{0\sigma} + X_i^{\sigma 0} (X_l^{00} + X_l^{\sigma\sigma}) X_m^{0\sigma} + X_i^{\tilde{\sigma} 0} X_l^{\sigma\tilde{\sigma}} X_m^{0\sigma} \right] - t_{im} X_i^{\sigma 0} (X_m^{00} + X_m^{\sigma\sigma}) X_l^{0\sigma} \right\}, \quad (32)$$

whereas the commutator of expression given by Eq. (30) with the spin part H_J of (1) is

$$[[S_m^z, H_J], H_J] = \frac{1}{8} \sum_{i,l,\sigma} J_{il} (J_{lm} - J_{im}) \times (S_m^\sigma S_i^z S_l^{\tilde{\sigma}} - S_m^\sigma S_i^{\tilde{\sigma}} S_l^z + S_i^z S_l^\sigma S_m^{\tilde{\sigma}} - S_i^{\tilde{\sigma}} S_l^z S_m^\sigma) + \frac{1}{8} \sum_{i,l,\sigma} J_{im} J_{lm} (2S_i^\sigma S_m^z S_l^{\tilde{\sigma}} - S_i^\sigma S_m^{\tilde{\sigma}} S_l^z - S_i^z S_m^\sigma S_l^{\tilde{\sigma}} + S_m^\sigma S_l^z S_i^{\tilde{\sigma}} - S_m^\sigma S_l^{\tilde{\sigma}} S_i^z + S_l^z S_i^\sigma S_m^{\tilde{\sigma}} - S_l^{\tilde{\sigma}} S_i^z S_m^\sigma). \quad (33)$$

The rest commutators of this type are as follows

$$[[S_m^z, H_J], H_t] = \frac{1}{4} \sum_{i,l,\sigma} \sigma \left[J_{im} t_{lm} (X_m^{\sigma 0} X_l^{\tilde{\sigma} 0} S_i^{\tilde{\sigma}} - S_i^\sigma X_m^{\tilde{\sigma} 0} X_l^{0\sigma} + S_i^\sigma X_l^{\tilde{\sigma} 0} X_m^{0\sigma} - X_l^{\sigma 0} X_m^{\tilde{\sigma} 0} S_i^{\tilde{\sigma}}) + (J_{im} - J_{lm}) t_{il} (S_m^\sigma X_i^{\tilde{\sigma} 0} X_l^{0\sigma} - X_i^{\sigma 0} X_l^{\tilde{\sigma} 0} S_m^{\tilde{\sigma}}) \right], \quad (34)$$

and

$$\begin{aligned}
[[S_m^z, H_t], H_J] = & \frac{1}{8} \sum_{i,l,\sigma} \sigma t_{im} \left[J_{il} (X_m^{\sigma 0} X_i^{0\tilde{\sigma}} S_l^{\tilde{\sigma}} \right. \\
& - X_m^{\sigma 0} X_i^{0\sigma} X_l^{\tilde{\sigma}\tilde{\sigma}} + X_i^{\tilde{\sigma} 0} S_l^{\sigma} X_m^{0\sigma} - X_i^{\sigma 0} X_l^{\tilde{\sigma}\tilde{\sigma}} X_m^{0\sigma} \\
& + X_m^{\sigma 0} S_l^{\tilde{\sigma}} X_i^{0\tilde{\sigma}} - X_m^{\sigma 0} X_l^{\tilde{\sigma}\tilde{\sigma}} X_i^{0\sigma} + S_l^{\sigma} X_i^{\tilde{\sigma} 0} X_m^{0\sigma} \\
& - X_l^{\tilde{\sigma}\tilde{\sigma}} X_i^{\sigma 0} X_m^{0\sigma}) - J_{lm} (X_m^{\tilde{\sigma} 0} S_l^{\sigma} X_i^{0\sigma} - X_m^{\sigma 0} X_l^{\tilde{\sigma}\tilde{\sigma}} X_i^{0\sigma} \\
& + X_i^{\sigma 0} X_m^{0\sigma} S_l^{\tilde{\sigma}} - X_i^{\sigma 0} X_m^{0\sigma} X_l^{\tilde{\sigma}\tilde{\sigma}} + S_l^{\sigma} X_m^{\tilde{\sigma} 0} X_i^{0\sigma} \\
& \left. - X_l^{\tilde{\sigma}\tilde{\sigma}} X_m^{\sigma 0} X_i^{0\sigma} + X_i^{\sigma 0} S_l^{\tilde{\sigma}} X_m^{0\tilde{\sigma}} - X_i^{\sigma 0} X_l^{\tilde{\sigma}\tilde{\sigma}} X_m^{0\sigma} \right]. \quad (35)
\end{aligned}$$

We conclude this subsection with the emphasis, that our Eqs. (31)-(35) are still exact. We will restrict further ourselves and take into account the correlations between the first and the second neighbors only. The resulting form of calculated commutators suggests the types of necessary thermodynamic averages. The calculation of these thermodynamic averages together with the decoupling procedures we need to employ in order to estimate the values of higher spin, transfer amplitude and density correlation functions will be presented in the following subsections.

B. Thermodynamic averages

To calculate the thermodynamic averages, we use the retarded Green's functions formalism. The equation of motion for a retarded Green's function $\langle\langle A|B \rangle\rangle_\omega$ takes the form

$$\omega \langle\langle A|B \rangle\rangle_\omega = \langle[A, B]_+\rangle + \langle\langle[A, H]|B \rangle\rangle_\omega, \quad (36)$$

where $\langle \dots \rangle$ denotes the thermal average. The standard relationship between correlation and Green's function may be written as

$$\langle BA \rangle = \frac{1}{2\pi i} \oint d\omega f(\omega) \langle\langle A|B \rangle\rangle_\omega, \quad (37)$$

where $f(\omega) = [\exp(\omega/k_B T) + 1]^{-1}$ is the Fermi function; the contour encircles the real axis without enclosing any poles of $f(\omega)$.

In general, Eq. (36) cannot be solved exactly and one needs some sort of approximation. To evaluate the Green's function $\langle\langle[A, H]|B \rangle\rangle_\omega$ in Eq. (36), one uses a decoupling scheme originally proposed by Roth³² for calculations on the Hubbard model. It can be shown that Roth's method is essentially equivalent to the Mori-Zwanzig projection technique^{33,34} and is strongly related to the moments method as applied to the evaluation of the spectral density of the Green's functions.^{35,36} Roth's method has been studied by many authors,^{34,37,38} and became a general method to treat approximately the quasiparticle spectrum of an interacting system. The reliability of the method has been demonstrated by comparison with the exact diagonalization results.³⁸

Roth's method³² implies that we seek a set of operators A_n , which are believed to be the most relevant to describe the one-particle excitations of the system of interest. Also, it is assumed that, in some approximation, these operators obey the relations³²

$$[A_n, H] = \sum_m K_{nm} A_m, \quad (38)$$

where the parameters K_{nm} are derived through a set of linear equations

$$\langle\langle[A_n, H], A_l]_+\rangle = \sum_m K_{nm} \langle\langle A_m, A_l^\dagger]_+\rangle. \quad (39)$$

Thus, it remains to define the operators A_n . Because, in the framework of the $t - J$ model, the quasiparticles are described by the Hubbard operators $X_{\mathbf{k}}^{0\sigma}$, a set of operators A_n contains only one operator $A = X_{\mathbf{k}}^{0\sigma}$. Hence, the matrix K_{nm} is diagonal and also contains one element $K = E_{\mathbf{k}}^\sigma$, where $E_{\mathbf{k}}^\sigma$ is the energy of of an electron with wave vector \mathbf{k} and spin projection σ . Consequently, Eqs. (38) and (39) become

$$[X_{\mathbf{k}}^{0\sigma}, H] = E_{\mathbf{k}}^\sigma X_{\mathbf{k}}^{0\sigma}, \quad (40)$$

$$\langle\langle[X_{\mathbf{k}}^{0\sigma}, H], X_{\mathbf{k}}^{\sigma 0}]_+\rangle = E_{\mathbf{k}}^\sigma \langle\langle X_{\mathbf{k}}^{0\sigma}, X_{\mathbf{k}}^{\sigma 0}]_+\rangle. \quad (41)$$

In the 2D $t - J$ model, long-range order is absent at any finite temperature and hence, $E_{\mathbf{k}}^\sigma$ does not depend on σ . Thus, we can replace $E_{\mathbf{k}}^+$ and $E_{\mathbf{k}}^-$ by $E_{\mathbf{k}}$.

For our evaluations we need the thermal averages of the following types: $\langle X_i^{\sigma 0} X_j^{0\sigma} \rangle$ and $\langle X_i^{\sigma\sigma} X_j^{\sigma'\sigma'} \rangle$. The averages (spin-spin correlation functions) of the type $\langle S_i^\sigma S_l^{\tilde{\sigma}} \rangle$ were defined in the SubSec. II B and the calculation procedure together with the numerical values will be outlined in the Sec. IV.

First, one should note, that in the absence of long-range order, $\langle X_i^{\tilde{\sigma}\tilde{\sigma}} \rangle$ does not depend on the site index and hence, according to Eq. (3), $T_0 = \langle X_i^{\tilde{\sigma}\tilde{\sigma}} \rangle = \langle X_i^{\sigma\sigma} \rangle = (1 - \delta)/2$ and $c_0 = \langle S_r^z S_r^z \rangle = 1/4$.

The transfer amplitude between the first neighbors $T_1 = pI_1$ is given by

$$T_1 = pI_1 = -\frac{1}{z} \sum_\rho \langle X_i^{\sigma 0} X_{i+\rho}^{0\sigma} \rangle \quad (42)$$

and may be calculated using the spectral theorem

$$I_1 = - \sum_{\mathbf{k}} \frac{\gamma_{\mathbf{k}}}{e^{\frac{E_{\mathbf{k}} - \mu}{k_B T}} + 1} \equiv \sum_{\mathbf{k}} \gamma_{\mathbf{k}} f_{\mathbf{k}}^h. \quad (43)$$

The parameter I_1 in Eq. (43) has been estimated in Ref. 21,

$$I_1 \approx \frac{4}{\pi} \left(1 - e^{-\pi\tilde{\delta}} \right) - 2\tilde{\delta}, \quad \tilde{\delta} = \frac{\delta}{1 + \delta}, \quad (44)$$

with an accuracy of a few percent over the whole region of δ from 0 to 1. Here one should note that for very small δ and low temperatures, $I_1 \approx 2\delta$.

The transfer amplitude between the second neighbors,

$$T_2 = \frac{1}{z(z-1)} \sum_{\rho \neq \rho'} \langle X_i^{\sigma 0} X_{i+\rho-\rho'}^{0\sigma} \rangle, \quad (45)$$

is

$$T_2 = \frac{p}{z(z-1)} \sum_{\mathbf{k}} \frac{16\gamma_{\mathbf{k}}^2 - 4 \cos k_x a \cos k_y a - 4}{e^{\frac{E_{\mathbf{k}} - \mu}{k_B T}} + 1} \\ \equiv -\frac{p}{z(z-1)} \sum_{\mathbf{k}} (16\gamma_{\mathbf{k}}^2 - 4 \cos k_x a \cos k_y a - 4) f_{\mathbf{k}}^h. \quad (46)$$

For p we have

$$p = \frac{1 + \delta}{2}, \quad (47)$$

where δ is the number of *extra* holes, due to doping, per one plane Cu^{2+} . The chemical potential μ is related to δ by

$$\delta = \frac{p}{N} \sum_{\mathbf{k}} f_{\mathbf{k}}^h. \quad (48)$$

where $f_{\mathbf{k}}^h = [\exp(-E_{\mathbf{k}} + \mu)/k_B T + 1]^{-1}$ is the Fermi function of holes.

To obtain the thermodynamic averages of the type $\langle X_i^{\sigma\sigma} X_{i+\rho}^{\sigma'\sigma'} \rangle$ it is convenient to make the following definitions

$$\lambda = \lambda_{\tilde{\sigma}\tilde{\sigma}} = \frac{1}{z} \sum_{\rho} \langle X_i^{\tilde{\sigma}\tilde{\sigma}} X_{i+\rho}^{\tilde{\sigma}\tilde{\sigma}} \rangle, \quad (49)$$

and

$$\lambda_{\sigma\sigma'} = \frac{1}{z} \sum_{\rho} \langle X_i^{\sigma\sigma} X_{i+\rho}^{\sigma'\sigma'} \rangle. \quad (50)$$

To obtain λ and $\lambda_{\sigma\tilde{\sigma}}$ we use the two Green's functions²¹

$$G_{\mathbf{k}}^{(1)}(\omega) = \frac{1}{z} \sum_{\rho} \langle \langle X_{\mathbf{k}}^{0\tilde{\sigma}} | X_i^{\tilde{\sigma}0} X_{i+\rho}^{\tilde{\sigma}\tilde{\sigma}} \rangle \rangle_{\omega}, \quad (51)$$

$$G_{\mathbf{k}}^{(2)}(\omega) = \frac{1}{z} \sum_{\rho} \langle \langle X_{\mathbf{k}}^{0\tilde{\sigma}} | X_i^{\tilde{\sigma}0} X_{i+\rho}^{\sigma\sigma} \rangle \rangle_{\omega}. \quad (52)$$

Note that in the paramagnetic state, $\lambda_{\sigma\sigma} = \lambda_{\tilde{\sigma}\tilde{\sigma}}$ and $\lambda_{\sigma\tilde{\sigma}} = \lambda_{\tilde{\sigma}\sigma}$.

According to Eqs. (36) and (40), the equation of motion for $G_{\mathbf{k}}^{(1)}(\omega)$ and $G_{\mathbf{k}}^{(2)}(\omega)$ can be written as

$$(\omega - E_{\mathbf{k}}) G_{\mathbf{k}}^{(1)}(\omega) = \frac{e^{i\mathbf{k}r_i}}{\sqrt{N}} (1 - p - \lambda_{\tilde{\sigma}\sigma} + pI\gamma_{\mathbf{k}}) \quad (53)$$

$$(\omega - E_{\mathbf{k}}) G_{\mathbf{k}}^{(2)}(\omega) = \frac{e^{i\mathbf{k}r_i}}{\sqrt{N}} (1 - p - \lambda_{\tilde{\sigma}\tilde{\sigma}}). \quad (54)$$

According to Eq. (37):

$$\lambda_{\tilde{\sigma}\tilde{\sigma}} = \frac{1}{2\pi i} \sum_{\mathbf{k}} \frac{e^{-i\mathbf{k}r_i}}{\sqrt{N}} \oint d\omega f(\omega) G_{\mathbf{k}}^{(1)}(\omega), \quad (55)$$

$$\lambda_{\tilde{\sigma}\sigma} = \frac{1}{2\pi i} \sum_{\mathbf{k}} \frac{e^{-i\mathbf{k}r_i}}{\sqrt{N}} \oint d\omega f(\omega) G_{\mathbf{k}}^{(2)}(\omega). \quad (56)$$

Consequently, Eqs. (53) and (54) lead to a system of linear equations for $\lambda_{\tilde{\sigma}\tilde{\sigma}}$ and $\lambda_{\tilde{\sigma}\sigma}$ with the trivial solution

$$\lambda = \lambda_{\tilde{\sigma}\tilde{\sigma}} = (1 - p)^2 - \frac{p^3}{2p - 1} I^2, \quad (57)$$

$$\lambda_{\sigma\tilde{\sigma}} = (1 - p - \lambda) \frac{1 - \delta}{1 + \delta} = (1 - p)^2 + \frac{(1 - p)p^2}{2p - 1} I^2. \quad (58)$$

C. Decoupling procedures

We now describe the decoupling procedures for the thermodynamic averages performed in spirit of Hubbard and Jain³⁹ and Kondo and Yamaji.²⁵

The averages of the type $\langle X_i^{\sigma 0} X_l^{0\sigma} X_m^{\tilde{\sigma} 0} X_j^{0\tilde{\sigma}} \rangle$ are decoupled resulting in products of transfer amplitudes and the decoupling parameter ζ ,

$$\langle X_i^{\sigma 0} X_l^{0\sigma} X_m^{\tilde{\sigma} 0} X_j^{0\tilde{\sigma}} \rangle \rightarrow \zeta \langle X_i^{\sigma 0} X_l^{0\sigma} \rangle \langle X_m^{\tilde{\sigma} 0} X_j^{0\tilde{\sigma}} \rangle. \quad (59)$$

The four-spin correlation functions are approximated, as usually, by products of two-spin correlation functions,¹⁶ however, multiplied now with the decoupling parameter ζ . Thus, we employ the decoupling procedures

$$\langle S_i^{\sigma} S_r^{\tilde{\sigma}} S_m^{\sigma} S_j^{\tilde{\sigma}} \rangle \rightarrow \zeta \langle S_i^{\sigma} S_r^{\tilde{\sigma}} \rangle \langle S_m^{\sigma} S_j^{\tilde{\sigma}} \rangle, \quad (60)$$

and

$$\langle S_i^z S_r^z S_m^{\sigma} S_j^{\tilde{\sigma}} \rangle \rightarrow \zeta \langle S_i^z S_r^z \rangle \langle S_m^{\sigma} S_j^{\tilde{\sigma}} \rangle, \quad (61)$$

for $i \neq r$ and $m \neq j$, whereas

$$\langle S_r^{\sigma} S_r^{\tilde{\sigma}} S_m^{\sigma} S_j^{\tilde{\sigma}} \rangle \rightarrow 2c_0 \langle S_m^{\sigma} S_j^{\tilde{\sigma}} \rangle. \quad (62)$$

The averages with the products of operators $X_i^{\sigma 0} X_r^{0\sigma}$ between the nearest(next-nearest) neighbors with $(1 - X_m^{\tilde{\sigma}\tilde{\sigma}})(1 - X_j^{\sigma'\sigma'})$ are decoupled as follows:

$$\langle X_i^{\sigma 0} X_r^{0\sigma} (1 - X_m^{\tilde{\sigma}\tilde{\sigma}})(1 - X_j^{\sigma'\sigma'}) \rangle$$

$$\rightarrow \langle X_i^{\sigma 0} X_r^{0\sigma} \rangle \langle 1 - X_m^{\tilde{\sigma}\tilde{\sigma}} - X_j^{\sigma'\sigma'} + X_m^{\tilde{\sigma}\tilde{\sigma}} X_j^{\sigma'\sigma'} \rangle. \quad (63)$$

and so on.

The averages with spin and Hubbard operators are decoupled as follows:

$$\langle X_i^{\sigma 0} X_j^{0\sigma} S_l^{\tilde{\sigma}} S_r^{\sigma} \rangle \rightarrow \langle X_i^{\sigma 0} X_j^{0\sigma} \rangle \langle S_l^{\tilde{\sigma}} S_r^{\sigma} \rangle, \quad (64)$$

and with spin and density operators:

$$\langle X_i^{\sigma\sigma} S_m^{\tilde{\sigma}} S_r^{\sigma} \rangle \rightarrow \langle X_i^{\sigma\sigma} \rangle \langle S_m^{\tilde{\sigma}} S_r^{\sigma} \rangle. \quad (65)$$

The averages $\langle X_i^{\sigma\sigma} X_j^{\sigma'\sigma'} \rangle$ between the second neighboring operators are decoupled simply by

$$\langle X_i^{\sigma\sigma} X_{i+2}^{\sigma'\sigma'} \rangle \rightarrow \langle X_i^{\sigma\sigma} \rangle \langle X_{i+2}^{\sigma'\sigma'} \rangle, \quad (66)$$

because an inspection of Eqs. (57) and (58) shows that the values of averages of these type between the first neighbors differ only slightly from $\langle X_i^{\sigma\sigma} \rangle \langle X_{i+\rho}^{\sigma'\sigma'} \rangle$. Therefore, the averages between second neighbors in Eq. (66) are thought as independent. In addition, because the averages $\langle X_i^{\sigma\sigma} X_j^{\sigma'\sigma'} \rangle$ between the first, in contrast to next-nearest, neighbors, are calculated exactly, the averages like $\langle X_r^{\sigma\sigma} X_m^{\sigma\sigma} X_j^{\sigma'\sigma'} \rangle$ are decoupled in a way to avoid, where possible, the averages of the type as given in Eq. (66).

D. Final result for $\langle \omega_{\mathbf{k}}^2 \rangle$ and $\langle \omega_{\mathbf{k}}^4 \rangle$

The expression for the second moment $\langle \omega_{\mathbf{k}}^2 \rangle$ is straightforward. Calculating the commutator with the expressions given by (30) and (31) with S_r^z , taking the thermal average and the Fourier transform, the result is

$$\langle \omega_{\mathbf{k}}^2 \rangle = -(8Jc_1 - 4t_{eff}pI_1)(1 - \gamma_{\mathbf{k}})/\chi(\mathbf{k}). \quad (67)$$

We now proceed with calculating the commutators for $\langle \omega_{\mathbf{k}}^4 \rangle$. Taking the commutators with the expressions given by Eqs. (32)-(35) with Eqs. (30) and (31) we obtain the expression for $\langle \omega_{\mathbf{k}}^4 \rangle$. The expression was then approximated using the decoupling procedures for thermal averages as was described in the previous SubSection. Taking the Fourier transform we arrive to expression that contains various types of sums over lattice sites. The corresponding types of sums over lattice sites are presented in Appendix A. Utilizing these sums we obtain

$$\begin{aligned} \langle \omega_{\mathbf{k}}^4 \rangle \simeq & -\left\{ 128J^3[c_2(1 - \gamma_{\mathbf{k}}^2)(\zeta c_2(\gamma_{\mathbf{k}} - \frac{3}{4}) - \frac{1}{4}c_0) \right. \\ & + c_0c_1(\frac{7}{4} - \frac{5}{2}\gamma_{\mathbf{k}} + \frac{3}{4}\gamma_{\mathbf{k}}^2) + \zeta c_1c_2(\frac{13}{4} - \frac{15}{2}\gamma_{\mathbf{k}} + \frac{17}{4}\gamma_{\mathbf{k}}^2) \\ & + \zeta c_1^2(\frac{3}{2} - \frac{43}{8}\gamma_{\mathbf{k}} + \frac{21}{4}\gamma_{\mathbf{k}}^2 + \frac{5}{8}\cos k_x a \cos k_y a - 2\gamma_{\mathbf{k}}^3)] \\ & + 16pI_1t_{eff}^3[c_1(3 - 2\gamma_{\mathbf{k}}^2 - \cos k_x a \cos k_y a) \\ & + \zeta T_2(7 - 12\gamma_{\mathbf{k}} + 5\gamma_{\mathbf{k}}^2) + \frac{1-\delta}{2}(1 - 4\gamma_{\mathbf{k}} + 3\gamma_{\mathbf{k}}^2) \\ & + (\delta + \lambda)(-\frac{9}{2} + 9\gamma_{\mathbf{k}} - 3\gamma_{\mathbf{k}}^2 - \frac{3}{2}\cos k_x a \cos k_y a)] \\ & + 16t_{eff}J^2pI_1[c_0(-\frac{39}{8} + \frac{31}{4}\gamma_{\mathbf{k}} - \frac{23}{8}\gamma_{\mathbf{k}}^2) \\ & + c_1(16\gamma_{\mathbf{k}}^3 - 35\gamma_{\mathbf{k}}^2 + 25\gamma_{\mathbf{k}} - \frac{9}{2} - \frac{3}{2}\cos k_x a \cos k_y a) \\ & + c_2(-\frac{85}{8} + \frac{93}{4}\gamma_{\mathbf{k}} - \frac{101}{8}\gamma_{\mathbf{k}}^2) + \frac{9}{16}\frac{1-\delta}{2}(\gamma_{\mathbf{k}} - 1)] \\ & + 16t_{eff}^2J[c_1(\frac{3}{4}\gamma_{\mathbf{k}} - \frac{3}{4}) + \frac{1+\delta}{2}c_1(6\gamma_{\mathbf{k}}^2 - \frac{45}{4}\gamma_{\mathbf{k}} + \frac{21}{4}) \\ & + T_2(\frac{1}{4}T_0 + \frac{3}{4}T_0^2 - \lambda)(2\gamma_{\mathbf{k}}^2 - 3\gamma_{\mathbf{k}} + 1) \\ & + (\frac{3}{4}\lambda^{+-}(1 - T_0) - T_0^2 + \lambda T_0)(\gamma_{\mathbf{k}} - 1) \\ & + \frac{1+\delta}{2}c_2(2\gamma_{\mathbf{k}}^2 - \frac{9}{2}\gamma_{\mathbf{k}} + \frac{5}{2}) + c_1T_0(\frac{9}{4}\gamma_{\mathbf{k}}^2 - \frac{5}{2}\gamma_{\mathbf{k}} + \frac{1}{4}) \\ & + c_1T_2(\frac{11}{4}\gamma_{\mathbf{k}}^2 - \frac{15}{2}\gamma_{\mathbf{k}} + \frac{19}{4}) \\ & + c_2T_0(-2\gamma_{\mathbf{k}}^2 + \frac{9}{2}\gamma_{\mathbf{k}} - \frac{5}{2}) \\ & + \zeta(pI_1)^2(-4\gamma_{\mathbf{k}}^3 + 6\gamma_{\mathbf{k}}^2 + \frac{11}{4}\gamma_{\mathbf{k}} - \cos k_x a \cos k_y a - \frac{15}{4}) \\ & + T_2c_2(16\gamma_{\mathbf{k}}^3 - 21\gamma_{\mathbf{k}}^2 - \frac{5}{2}\gamma_{\mathbf{k}} + \frac{15}{2}) \\ & + T_0T_2(2\gamma_{\mathbf{k}}^2 - \frac{9}{2}\gamma_{\mathbf{k}} + \frac{5}{2}) + T_2c_0(-5\gamma_{\mathbf{k}}^2 + \frac{9}{2}\gamma_{\mathbf{k}} + \frac{1}{2}) \\ & \left. + \zeta T_2^2(-2\gamma_{\mathbf{k}}^3 + 6\gamma_{\mathbf{k}}^2 - \frac{19}{4}\gamma_{\mathbf{k}} + \frac{3}{4})\right\}/\chi(\mathbf{k}). \quad (68) \end{aligned}$$

To insure the accuracy of the calculations we compare the result for spin part H_J with that reported in the

literature.¹⁶ One should note that $[S_m^z, n_i] = 0$. Thus, the commutator (30) does not depend on the density-density term $n_i n_j$ in (1). Moreover, the commutator of spin operators S_m^σ appearing in (30) with the density operators n_i is zero also: $[S_m^\sigma, n_i] = 0$. This enables us to compare the result (68) for spin part with the results for carrier free 2DHAF. As it was already mentioned, we restrict ourselves and take into account the correlations between the first and the next-nearest neighbors only.

For the second moment $\langle \omega_{\mathbf{k}}^2 \rangle$ the result (67) is evidently correct. To compare the results for $\langle \omega_{\mathbf{k}}^4 \rangle$ we need some additional effort. The corresponding expressions and the procedure will be described in Appendix B. The expression, as shown in (68), with $t_{eff} = 0$ and with the decoupling parameter ζ settled to unity $\zeta = 1$ is the same, as given in Ref. 16 and may be compared using the integrals (sums) over the Brillouin zone (see Appendix B).

IV. COMPARISON WITH EXPERIMENT AND DISCUSSION

The results of the calculations are summarized in the Table 1. The value of *extra* holes, due to doping, per one plane Cu^{2+} , δ , can be identified with the Sr content x in $\text{La}_{2-x}\text{Sr}_x\text{CuO}_4$. The AF spin-spin correlation functions c_1 , c_2 , the spin stiffness constant ρ_S and the parameter g_- were calculated using the expressions and the procedure as described in Ref. 17 (see also Ref. 21) in the $T \rightarrow 0$ limit, since we will employ them in a temperature range $T < 1000$ K $\simeq 0.7 J$, where experimental data exist and according to the calculations their values have a weak temperature dependence.

Table 1. The calculated at $T \rightarrow 0$ values of AF spin-spin correlation function c_1 between the first neighbors, the g_- parameter and the spin stiffness constant ρ_S as a function of $\text{La}_{2-x}\text{Sr}_x\text{CuO}_4$ doping x together with the values of decoupling parameter ζ as extracted from comparison with ^{63}Cu NQR spin-lattice relaxation rate measurements.

x	c_1	g_-	$2\pi\rho_S/J$	ζ
0	- 0.115215	4.1448	0.38	1.8
0.012	- 0.11474	4.137	0.37	1.8
0.02	- 0.11391	4.117	0.365	-
0.024	- 0.11333	4.102	0.36	1.6
0.03	- 0.11238	4.080	0.355	1.5
0.035	- 0.11152	4.060	0.35	~ 1.3
0.04	- 0.11057	4.037	0.345	1.1

A. Temperature and doping dependence of antiferromagnetic correlation length

The AF correlation length, its doping and temperature dependence is given by Eq. (25). ξ_0 is the value of correlation length at $T = 0$ and gives information on the topology of holes. At present, two types of doping dependencies are under debate in the literature. The first,⁴⁰ is the localization of holes close to the randomly distributed Sr^{2+} ions gives $\xi_0 = a/\sqrt{x}$. The other one is the formation of dynamic domain walls. In this case $\xi_0 = a/nx$, where n is the average distance between the holes along the domain walls in lattice units,^{41,42} usually called "stripes".

The best fit of ξ_{eff} to experimental data²⁶ yields $\xi_0 = a/nx$, where $n = 1.3$ for samples with $x \lesssim 0.02$ and $n = 2$ for samples with $x > 0.02$, see Figure 1. These results are in agreement with the conclusion of Borsa *et al.*⁴¹ for $\text{La}_{2-x}\text{Sr}_x\text{CuO}_4$ compounds with $x \lesssim 0.02$ and with the analysis of Carretta *et al.* on the basis of dynamical scaling.⁴³ The presence of stripes with $n = 2$ was found also by Tranquada *et al.* in $x \simeq 1/8$ compound.⁴²

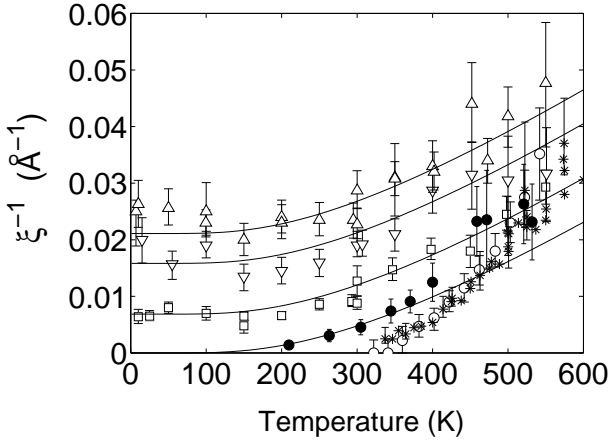


FIG. 1. The inverse correlation length ξ_{eff} versus temperature fitted (solid lines) to the experimental data as obtained from neutron scattering experiments. For carrier free La_2CuO_4 : filled circles from Ref. 4 (the fitted data), asterisks from Ref. 44 and open circles from Ref. 26. For doped $\text{La}_{2-x}\text{Sr}_x\text{CuO}_4$: squares for $x = 0.02$, down triangles for $x = 0.03$ and up triangles for $x = 0.04$ from Ref. 26.

The fit with the relation a/nx in ξ_0 may be obtained by comparing the experimental data in the low temperature region. Indeed, the doping relation a/\sqrt{x} fits with the neutron scattering data poorly than the a/nx does, keeping in mind the value of plane lattice constant $a = 3.79$ Å. For example, for $x = 0.02$ one has $\xi_0^{-1} = \sqrt{x}/3.79 = 0.037$ Å⁻¹ whereas the experimental value is 0.005–0.007 Å⁻¹. The inability to fit the $1/\sqrt{x}$ relation within the NS data²⁶ is clear also for larger values of doping: $\xi_0^{-1} = \sqrt{x}/3.79 = 0.046$ Å⁻¹ for $x = 0.03$ and $\xi_0^{-1} = \sqrt{x}/3.79 = 0.053$ Å⁻¹ for $x = 0.04$ differs strongly from 0.013–0.02 Å⁻¹ and 0.02–0.026 Å⁻¹, consequently, as obtained by NS²⁶ (see Fig. 1). On the other hand, the relation $\xi_0^{-1} = nx/a$ gives good agreement: 0.0069 Å⁻¹ for $x = 0.02$ with $n = 1.3$, and 0.016 Å⁻¹

for $x = 0.03$, and 0.021 Å⁻¹ for $x = 0.04$ with $n = 2$. The value $n = 1.3$ for $x = 0.02$ fits the values of correlation length as obtained from experimental data better in contrast to that with $n = 2$. This result is especially evident when one tries to compare the values of ξ_{eff}^{-1} at high temperatures. The high quality of the fit is in agreement with previous studies and seems to confirm the microsegregation, however, with different values of average distance between the holes along the domain walls. It is tempting to speculate that the change in the average distance n from $n \approx 1.3$ for $x \lesssim x_c$ and $n = 2$ for $x > x_c$ appears at the value of Sr content when the Néel order is completely suppressed ($T_N \rightarrow 0$ at $x = x_c \simeq 0.02$) as discussed, consequently, for example, in Refs. 41 and 45.

Having established the temperature and doping dependence of correlation length we now proceed with calculations of the nuclear spin-lattice relaxation rate.

B. Spin-diffusion constant

The spin-diffusion is described by the $(\mathbf{k}, \omega) = (0, 0)$ mode. The spin-diffusion plays an important role in an antiferromagnet and makes a pronounced contribution to the relaxation rates. The spin-diffusion constant D is given by⁴⁶

$$D = \lim_{k \rightarrow 0} \frac{1}{\pi k^2 F(\mathbf{k}, 0)} = \lim_{k \rightarrow 0} \frac{1}{k^2} \sqrt{\frac{\pi \langle \omega_{\mathbf{k}}^2 \rangle^3}{2 \langle \omega_{\mathbf{k}}^4 \rangle}}. \quad (69)$$

For small \mathbf{q} , $\Delta_{1\mathbf{q} \rightarrow 0}^2$ tends to zero as

$$\Delta_{1\mathbf{q} \rightarrow 0}^2 = -(q_x^2 a^2 + q_y^2 a^2)(2Jc_1 - t_{eff}pI_1)/\chi_S, \quad (70)$$

whereas $\Delta_{2\mathbf{q} \rightarrow 0}^2 \simeq \langle \omega_{\mathbf{q} \rightarrow 0}^4 \rangle / \langle \omega_{\mathbf{q} \rightarrow 0}^2 \rangle$ remains finite,

$$\begin{aligned} \Delta_{2\mathbf{q} \rightarrow 0}^2 = & \left\{ 128J^3 \left[\frac{1}{8}c_2(\zeta c_2 - c_0) - \frac{1}{4}\zeta c_1 c_2 + \frac{1}{4}c_0 c_1 \right. \right. \\ & - \left. \frac{3}{32}\zeta c_1^2 \right] + 16pI_1 t_{eff}^3 \left(\frac{3}{2}c_1 + \frac{1}{2}\zeta T_2 - \frac{1}{2}\frac{1-\delta}{2} \right) \\ & + 16t_{eff}J^2 pI_1 \left(\frac{1}{2}c_2 - \frac{1}{2}c_0 - \frac{9}{64}\frac{1-\delta}{2} \right) \\ & + 16t_{eff}^2 J \left[-\frac{3}{16}\frac{1+\delta}{2}c_1 - \frac{1}{4}T_2 \left(\frac{1}{4}T_0 + \frac{3}{4}T_0^2 - \lambda \right) \right. \\ & - \frac{1}{4} \left(\frac{3}{4}\lambda^{+-}(1 - T_0) - T_0^2 + \lambda T_0 \right) + \frac{1}{8}\zeta \frac{1+\delta}{2} - \frac{3}{16}c_1 \\ & - \frac{1}{2}c_1 T_0 - \frac{1}{8}c_2 T_0 - \frac{3}{16}\zeta (pI_1)^2 + \frac{1}{2}c_1 T_2 - \frac{7}{8}T_2 c_2 \\ & \left. \left. + \frac{1}{8}T_2 T_0 + \frac{11}{8}T_2 c_0 - \frac{5}{16}\zeta T_2^2 \right] \right\} / \left\{ 2Jc_1 - t_{eff}pI_1 \right\}. \quad (71) \end{aligned}$$

The values of D for carrier free AF system may be compared with the results of other theories. The infinite temperature result is the same as in Ref. 19, namely $D(T \rightarrow \infty) = \frac{1}{8}\sqrt{2\pi}Ja^2 = 0.3133Ja^2$. This value is close to that obtained by Morita,⁴⁷ $D = 0.43Ja^2$ and $D = \frac{1}{10}\sqrt{5\pi}Ja^2 = 0.3963Ja^2$ in Refs. 23, 48, 49. The calculated value of $D = 2.46Ja^2$ at $T \rightarrow 0$ (with $\zeta = 1$) is larger compared to that obtained in Ref. 19, $D = 1.63Ja^2$. The value of $D = 2.66Ja^2$ (with $\zeta = 1.8$) is compatible with $D \approx 3Ja^2$ obtained at $T = 900$ K in

Ref. 48. In general, D weakly changes with doping and when one vary ζ . Figure 2 shows the doping dependence of D for two cases, with $\zeta = 1$ and when ζ is obtained from the best fit to NQR data. The calculated doping dependence of D in the $T \rightarrow 0$ limit may be compared with the results of Bonca and Jaklic⁵⁰ at high temperatures, assuming that the doping dependence of D remains the same. Indeed, Figure 2 shows the remarkable agreement.

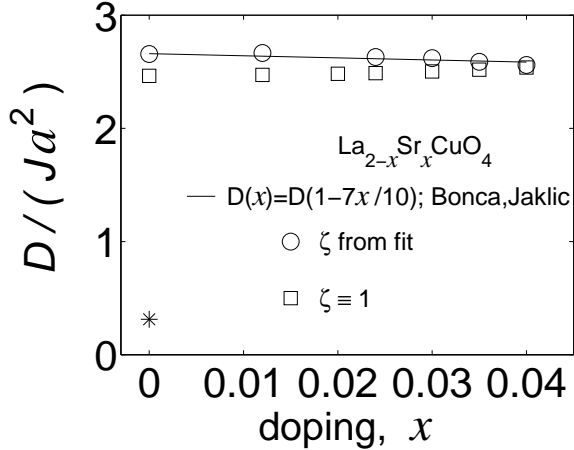


FIG. 2. The calculated doping dependence of the spin diffusion constant D in the $T \rightarrow 0$ limit with the fixed decoupling parameter $\zeta = 1$ (squares) and with ζ as obtained from the best fit to NQR data (circles). The solid line is the result of Bonca and Jaklic⁵⁰ for doping dependence of D in the high temperature limit. The asterisk marks the value of the spin diffusion constant D in the limit of high temperatures $T \rightarrow \infty$.

C. Dynamic structure factor

Now, since the nuclear spin-lattice relaxation rate is determined by the dynamic structure factor $S(\mathbf{q}, \omega)$ we first consider its temperature, frequency and wavevector dependence. First, we note that for all temperatures the relaxation shape function $F(\mathbf{q}, \omega)$ as well as $S(\mathbf{q}, \omega)$ give the elastic peak at $q = 0$ and $\omega = 0$. This is clear from Eq. (17) since both $\langle \omega_{\mathbf{q}}^2 \rangle$ and $\langle \omega_{\mathbf{q}}^4 \rangle \sim q^2$ for small q . We now turn to the case of finite but small NMR/NQR frequencies.

The relaxation shape function $F(\mathbf{k}, \omega)$ with small ω , compared to temperature scale of the system, related to $S(\mathbf{k}, \omega)$ as

$$S(\mathbf{k}, \omega \sim 0) = 2\pi k_B T \chi(\mathbf{k}) F(\mathbf{k}, \omega), \quad (72)$$

We now explore the form of $S(\mathbf{k}, \omega)$ and obtain two peaks: one at $\mathbf{q} \sim 0$ and the other at $\mathbf{Q} = (\pi/a, \pi/a)$. The $S(\mathbf{q}, \omega)$ value at small \mathbf{q} is large when the \mathbf{q} values are such that

$$\Delta_{1\mathbf{q}}^2 \simeq \omega \tau_{\mathbf{q}} \Delta_{2\mathbf{q}}^2, \quad (73)$$

see Eqs. (17), (18), and (70), (71). Thus, $S(\mathbf{q}, \omega)$ has a sharp peak at \mathbf{q}_0 :

$$S(\mathbf{q}_0, \omega) = \frac{k_B T \chi_S}{\omega}, \quad (74)$$

and the $S(\mathbf{k}, \omega)$ value at $\mathbf{Q} = (\pi/a, \pi/a)$ is given by

$$S(\mathbf{Q}, \omega) \simeq \frac{2k_B T \chi(\mathbf{Q}) \tau_{\mathbf{Q}} \Delta_{2\mathbf{Q}}^2}{\Delta_{1\mathbf{Q}}^2}. \quad (75)$$

The relation given in Eq. (74) is in agreement with the result of Makivić and Jarrel⁵¹ on frequency dependence of the dynamic structure factor at small values of wavevectors as extracted from combination of the Maximum Entropy Method and Quantum Monte Carlo calculations. This result agrees also with the basic relations known in the literature. From general physical grounds, namely, linear response theory, hydrodynamics and fluctuation-dissipation theorem, the diffusive spin dynamics gives the form of dynamic structure factor⁵²

$$S(\mathbf{q} \sim 0, \omega \sim 0) \simeq \frac{2\chi_S}{1 - \exp(-\omega/k_B T)} \times \frac{\omega D \mathbf{q}^2}{\omega^2 + (D \mathbf{q}^2)^2}, \quad (76)$$

for small \mathbf{q} and ω .

Using Eq. (76) (or, equivalently, from Eq. (73)) one may easily estimate the value of \mathbf{q}_0 which is given by

$$q_0^2 \simeq \omega/D. \quad (77)$$

For typical value of the measuring frequency, $\omega \approx 1$ mK, $q_0 a \approx \pi \times 10^{-4}$ and weakly changes when one varies doping and the decoupling parameter ζ ($q_{0x} = q_{0y} = \frac{1}{\sqrt{2}} q_0$).

For small $\mathbf{q} \ll \mathbf{q}_0$ with finite ω the relaxation shape function $F(\mathbf{q}, \omega)$ and the dynamic structure factor $S(\mathbf{q}, \omega)$ approaches zero: $S(\mathbf{q}_0 \gg \mathbf{q} \rightarrow 0, \omega) \rightarrow 0$.

Thus, the contribution to the nuclear relaxation rates from \mathbf{q} around 0 has no peculiarities since ω is finite, but small, compared to any values of the variables (we use $J = 0.12$ eV (1393 K)). Figures (3)-(10) show the calculated dynamic structure factor for different values of doping, temperature and decoupling parameter ζ with $\omega_c = 2\pi \times 33$ MHz ($= 1.365 \times 10^{-7}$ eV) and with $\omega_0 = 2\pi \times 52$ MHz ($= 2.15 \times 10^{-7}$ eV) for $x = 0.035$.

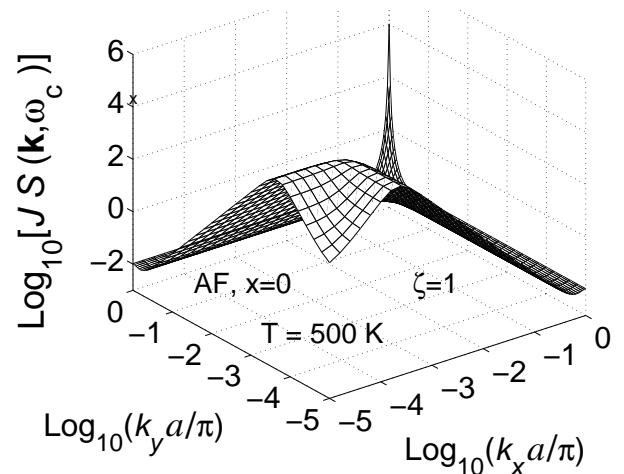


FIG. 3. Log-scale mesh of the calculated dynamic structure factor $S(\mathbf{k}, \omega_c)$ for carrier free antiferromagnet at $T = 500$ K with simple decoupling $\zeta = 1$. The cross on the vertical axis marks the maximum of $J S(\mathbf{k}, \omega_c)$ at $\mathbf{k} = \mathbf{q}_0$.

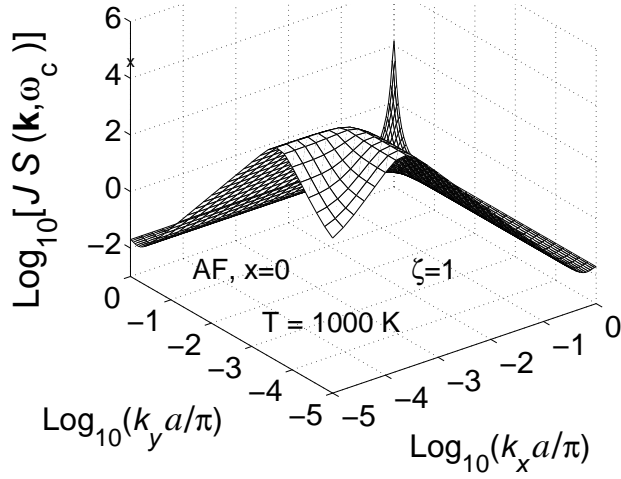


FIG. 4. Log-scale mesh of the calculated dynamic structure factor $S(\mathbf{k}, \omega_c)$ for carrier free antiferromagnet at $T = 1000$ K with simple decoupling $\zeta = 1$. The cross on the vertical axis marks the maximum of $JS(\mathbf{k}, \omega_c)$ at $\mathbf{k} = \mathbf{q}_0$.

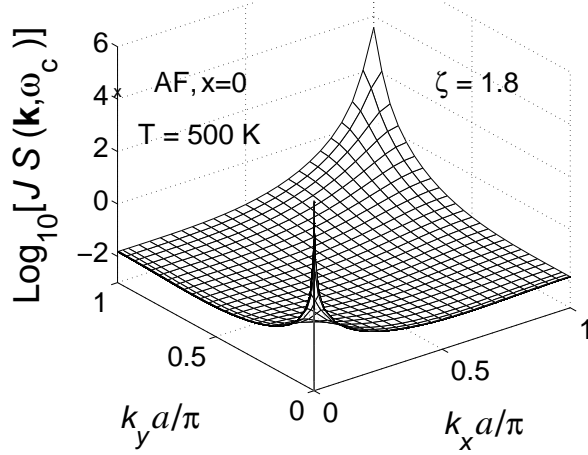


FIG. 5. Semilog-scale mesh of the calculated dynamic structure factor $S(\mathbf{k}, \omega_c)$ for carrier free antiferromagnet at $T = 500$ K with the decoupling parameter $\zeta = 1.8$. The region of small \mathbf{q} values ($\mathbf{q} \ll \mathbf{q}_0$) for which $\text{Log}_{10}[JS(\mathbf{k}, \omega)] < -3$ is not shown. The cross on the vertical axis marks the maximum of $JS(\mathbf{k}, \omega_c)$ at $\mathbf{k} = \mathbf{q}_0$.

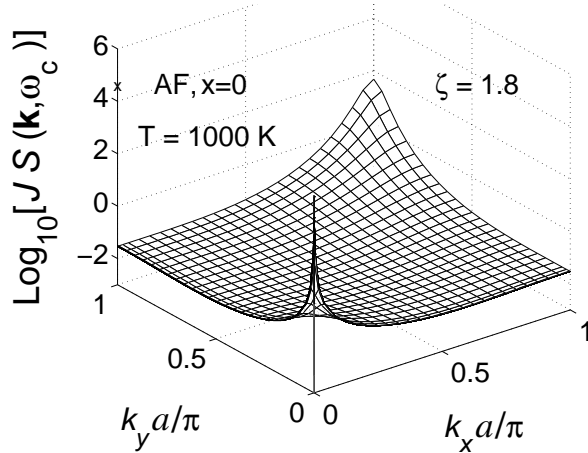


FIG. 6. Semilog-scale mesh of the calculated dynamic structure factor $S(\mathbf{k}, \omega_c)$ for carrier free antiferromagnet at $T = 1000$ K with the decoupling parameter $\zeta = 1.8$. The region of small \mathbf{q} values ($\mathbf{q} \ll \mathbf{q}_0$) for which $\text{Log}_{10}[JS(\mathbf{k}, \omega)] < -3$ is not shown. The cross on the vertical axis marks the maximum of $JS(\mathbf{k}, \omega_c)$ at $\mathbf{k} = \mathbf{q}_0$.

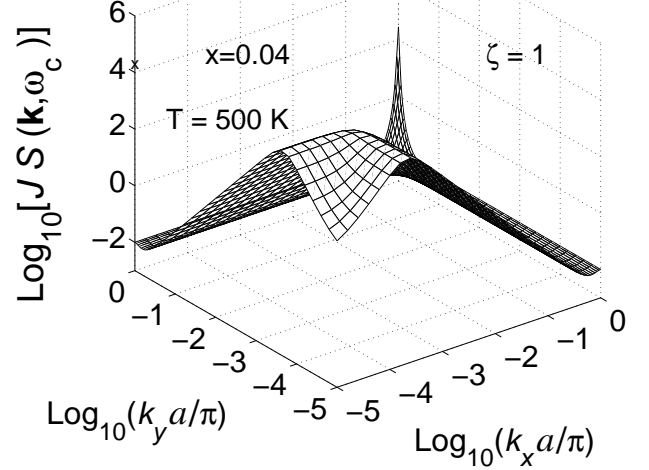


FIG. 7. Log-scale mesh of the calculated dynamic structure factor $S(\mathbf{k}, \omega_c)$ for $x = 0.04$ hole content at $T = 500$ K with simple decoupling $\zeta = 1$. The cross on the vertical axis marks the maximum of $JS(\mathbf{k}, \omega_c)$ at $\mathbf{k} = \mathbf{q}_0$.

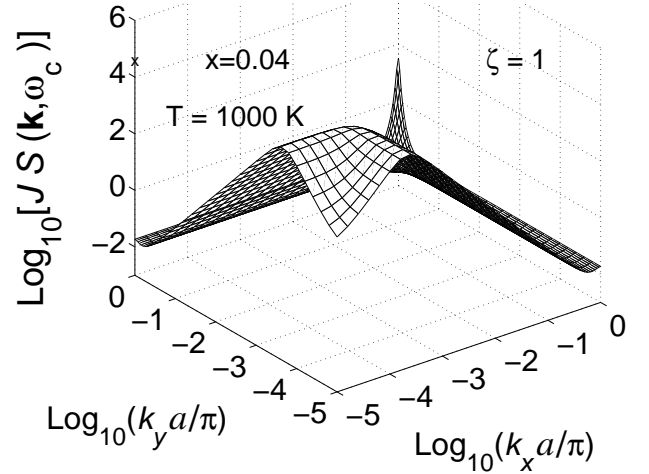


FIG. 8. Log-scale mesh of the calculated dynamic structure factor $S(\mathbf{k}, \omega_c)$ for $x = 0.04$ hole content at $T = 1000$ K with simple decoupling $\zeta = 1$. The cross on the vertical axis marks the maximum of $JS(\mathbf{k}, \omega_c)$ at $\mathbf{k} = \mathbf{q}_0$.

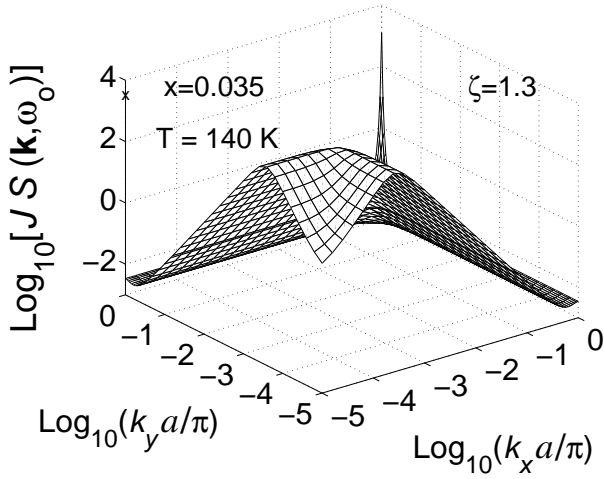


FIG. 9. Log-scale mesh of the calculated dynamic structure factor $S(\mathbf{k}, \omega_0)$ for $x = 0.035$ hole content at $T/J = 0.1$ ($T \simeq 140$ K) with simple decoupling $\zeta = 1$. The cross on the vertical axis marks the maximum of $JS(\mathbf{k}, \omega_0)$ at $\mathbf{k} = \mathbf{q}_0$.

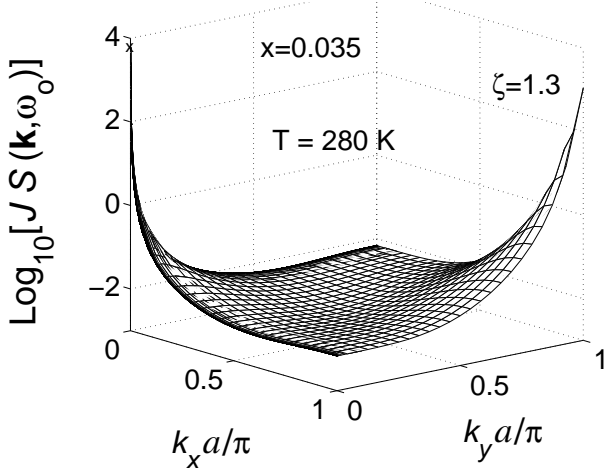


FIG. 10. Semilog-scale mesh of the calculated dynamic structure factor $S(\mathbf{k}, \omega_0)$ for $x = 0.035$ hole content at $T/J = 0.2$ ($T \simeq 280$ K). The region of small \mathbf{q} values ($\mathbf{q} \ll \mathbf{q}_0$) for which $\text{Log}_{10}(JS(\mathbf{k}, \omega)) < -3$ is not shown. The cross on the vertical axis marks the maximum of $JS(\mathbf{k}, \omega_0)$ at $\mathbf{k} = \mathbf{q}_0$.

D. Nuclear spin-lattice relaxation

The nuclear spin-lattice relaxation rate ${}^\alpha(1/T_1)$ is given by

$${}^\alpha(1/T_1) = \frac{1}{\pi} \sum_{\mathbf{k}} {}^\alpha F(\mathbf{k})^2 S(\mathbf{k}, \omega), \quad (78)$$

where ω is the measuring NMR/NQR frequency, ${}^\alpha F(\mathbf{k})$ is the wave vector dependent hyperfine formfactor^{53,54}

$${}^{17}F(\mathbf{k})^2 = 2C^2 (1 + \gamma_{\mathbf{k}}), \quad (79)$$

for planar ${}^{17}\text{O}$ and

$${}^{63}F(\mathbf{k})^2 = (A_{ab} + 4\gamma_{\mathbf{k}}B)^2, \quad (80)$$

for ${}^{63}\text{Cu}$ sites. A_{ab} and B are the Cu on-site and transferred hyperfine couplings, respectively. The quantization axis of the electric field gradient coincides with

the crystal axis c which is perpendicular to CuO_2 planes defined by a and b . For C in Eq. (79), we adopted the formula $C^2 = \frac{1}{6}(C_{\parallel}^2 + C_{\perp}^2)$, where C_{\parallel} and C_{\perp} are the plane oxygen hyperfine couplings for two axis perpendicular to c , and that includes the factor $\frac{1}{3}$ to account ${}^{17}(1/T_1)$ as measured by NMR. The values of hyperfine couplings were taken as follows: $A_{ab} = 3.7 \times 10^{-7}$ eV, for transferred hyperfine coupling B the relation $B = (1 + 2.75x) \times 3.8 \times 10^{-7}$ eV is used to match the weak changes with Sr doping⁵⁵ and $C = 2.8 \times 10^{-7}$ eV in accord with the values as extracted from NMR data and used in calculations of relaxation rates.^{1,11,19,43,45,48,53-56}

The ${}^{17}\text{O}$ and ${}^{63}\text{Cu}$ nuclear relaxation rates are essentially determined by the corresponding formfactors given by Eqs. (79) and (80). Figures 11 and 12 show the quantity ${}^\alpha F(\mathbf{k})^2 S(\mathbf{k}, \omega)$ in a log-scale plot *versus* k_x ($k_y = 0$) and a semilog-scale plot along the diagonal of the Brillouin zone. The calculations show the $1/\mathbf{k}^2$ wavevector dependence of $S(\mathbf{k}, \omega)$ for $\mathbf{k} > \mathbf{q}_0$ and the \mathbf{k}^2 dependence of $S(\mathbf{k}, \omega)$ for $\mathbf{k} < \mathbf{q}_0$. The form of ${}^\alpha F(\mathbf{k})^2 S(\mathbf{k}, \omega)$ gives the peaks at \mathbf{q}_0 and $\mathbf{k} \simeq (\pi/a, \pi/a)$. Thus, two types of contributions dominate in the nuclear spin-lattice relaxation rates.

Here one should note, that the theory contains the decoupling procedures for correlation functions and the decoupling parameter ζ has been introduced. In general, despite the complicated structure of $\langle \omega_{\mathbf{k}}^4 \rangle$, ζ allows to regulate the contributions with $\mathbf{k} \simeq (\pi/a, \pi/a)$ to the spin-lattice relaxation rate $1/T_1$. The larger ζ , the smaller is the contribution from $\mathbf{k} \simeq (\pi/a, \pi/a)$ to $1/T_1$.

The contribution to $1/T_1$ from \mathbf{q} around 0 has no peculiarities because the measuring frequency is *finite* ($\omega_c \approx 2\pi \times 33$ MHz ($= 1.58$ mK) in ${}^{63}\text{Cu}$ NQR and $\omega_0 \approx 2\pi \times 52$ MHz ($= 2.5$ mK) in ${}^{17}\text{O}$ NMR measurements), but small, compared to any values of the variables (we take $J = 0.12$ eV (1393 K)). The calculations also show that ${}^\alpha F(\mathbf{k})^2 S(\mathbf{k}, \omega)$ has a broad local minimum at \mathbf{q}_m which values are given by $q_{xm}^2 + q_{ym}^2 \approx \pi^2/a^2$.

A direct numerical integration over \mathbf{k} is difficult, because ${}^\alpha F(\mathbf{k})^2 S(\mathbf{k}, \omega)$ has an extremely sharp peak at very small \mathbf{q}_0 . This requires an unattainably large number of points in numerical integration over Brillouin zone.

We first estimate the value of contribution to $1/T_1$ from small \mathbf{q} because Figures (11), (12) show that the pronounced contribution to relaxation rates should come from excitations with $q \sim 0$. In the formulation of Ref. 10, the diffusive contribution,

$$\text{Chakravarty } (1/T_1)_{\text{Diff}} \sim \sum_{\mathbf{q} \sim 0} \frac{T \chi S}{D q^2} \quad (81)$$

is divergent. While usually, this logarithmic divergence of $(1/T_1)_{\text{Diff}}$ was argued to cut off,^{10,48} since in a real systems the mechanism destroying the diffusion should be taken into account. In $\text{La}_{2-x}\text{Sr}_x\text{CuO}_4$ the combination of three-dimensional effects, finite length scale and the presence of disorder in CuO_2 planes may suppress the effect of spin diffusion on spin-lattice relaxation rates. For example, using exact diagonalization technique in the high temperature region, it was argued that strong local perturbation induced by oxygen defects limit the spin-diffusion.⁴⁸ Despite of considerable effort, the appropri-

ate account of these effects is still unavailable because of lack of any exact analytical result.

In the present theory the meaning of q_0 is clear: it is the value of \mathbf{k} at which the maximum in $S(\mathbf{k}, \omega)$ occurs and for small ω it may be treated as the cut off in the integration for calculation of the contribution from spin diffusion (see Eq. (81) and Ref. 10). For $\mathbf{q} \ll \mathbf{q}_0$ the integration over \mathbf{q} should be taken over the factor $\sim \mathbf{q}^2/\mathbf{q}_0^2$. One should note, that in the present theory the form of the calculated dynamic structure factor $S(\mathbf{k}, \omega)$ comes *not from, e.g., disorder*, but rather than from the relaxation function and is in *agreement* with linear response theory, hydrodynamics and fluctuation-dissipation theorem and this result does not depend on the order of the pole approximation in the relaxation function theory.

Expanding $S(\mathbf{q}, \omega)$ around q_0 we obtain,

$$\alpha(1/T_1)_{Diff} = \frac{\alpha F(0)^2 k_B T a^2 \chi_S}{\pi \hbar D} \Lambda, \quad (82)$$

where Λ depends on frequency through q_0 . A simple and rough estimate gives

$$\Lambda \sim \ln(1/q_0^2) \sim \ln(const \times J/\omega). \quad (83)$$

This result explains the reason why the oxygen $^{17}(1/T_1)$ relaxation rate as measured by NMR remains unchanged at 9 T ($\omega_0 = 2\pi \times 52$ MHz) and 14.1 T ($\omega_0 = 2\pi \times 81.4$ MHz) within the experimental accuracy.⁵⁷ One should note that ω is much less than $J = 1.8 \times 10^8$ MHz, hence $\ln(J/52 \text{ MHz})/\ln(J/81.4 \text{ MHz}) \approx 1.03$. Indeed, a sophisticated calculation gives $\Lambda(33 \text{ MHz}) = 2.52$, $\Lambda(52 \text{ MHz}) = 2.44$, and $\Lambda(81.4 \text{ MHz}) = 2.37$ and its value changes on less than 1% when one vary ζ and doping within $x \lesssim 0.04$. In view of the result that the spin diffusion contribution is 70 %, the relative shift of the measured $^{17}(1/T_1)$ will be ≈ 2 %, that lies within the experimental error (see Figure 13).

The $^{17}(1/T_1)$ relaxation rate has a contribution due antiferromagnetic correlations between copper spins, however, for wave vectors only in the vicinity of $\mathbf{Q} = (\pi/a, \pi/a)$ because the formfactor $^{17}F(\mathbf{k})$ filters out the contributions with $\mathbf{Q} = (\pi/a, \pi/a)$. This filter causes also the minor sensitivity to the decoupling parameter ζ . The value of $\zeta = 1.3$ for $x = 0.035$ (see Table 1) is a plausible guess. This contribution was calculated by direct summation over \mathbf{k} in the region $\mathbf{k} > \mathbf{q}_m$.

Figure 13 shows the calculated ^{17}O relaxation rate in the sector of lightly damped spin waves at low temperatures. It is seen that ^{17}O relaxation rate has a weak frequency dependence. The good agreement of calculations (even without adjusting the parameter ζ) with experiment shows, that in case the mechanism destroying the diffusion is present in $\text{La}_{2-x}\text{Sr}_x\text{CuO}_4$, whether it is caused by the three-dimensional effects, finite length scale or the presence of disorder in CuO_2 planes, it seems that it affects the spin-lattice relaxation rates only little through the contribution from spin diffusion.

A fair agreement between experiment and calculated $^{17}(1/T_1)$ for lightly doped $\text{La}_{2-x}\text{Sr}_x\text{CuO}_4$ may be thought as fortuitous because of the following reason. In the present theory, the contribution to relaxation rate from small \mathbf{q} depends on spin diffusion constant D as,

$$(1/T_1)_{Diff} \sim \frac{1}{D} \ln(const \times D/\omega). \quad (84)$$

In the $T \rightarrow 0$ limit the spin diffusion constant D has to diverge for both carrier free and lightly doped $\text{La}_{2-x}\text{Sr}_x\text{CuO}_4$ since both Heisenberg and $t - J$ models have nonzero spin stiffness.⁵⁰ On the other hand, in the quantum critical region, $\rho_S < T < J$ (note that in the present theory $\rho_S \simeq 0.06J \approx 80$ K and weakly decreases with light doping), the spin-diffusion constant scales as $D \sim T^{1/2}\xi$ (see Ref. 3). For lightly doped $x \approx 0.03$ systems one may expect this scaling to be valid also, but with finite correlation length for $T \gtrsim \rho_S$ (see Figure 1). This justifies the validity of the present formulation and the propriety of the results obtained for *finite* doping and low temperatures.

It is worth to mention the results of calculations by Chakravarty *et al.*^{9,59,60} of relaxation rates for La_2CuO_4 on various nuclei. The results of CHN gave the temperature dependence of correlation length with the two-loop corrections in perfect agreement with experiment. The calculated plane copper relaxation rate $^{63}(1/T_1)$ within the CHN theory is in agreement with experiment,⁵⁸ however, for plane oxygen the results of calculations does not reproduce the values of the measured $^{17}(1/T_1)$ for insulating $\text{Sr}_2\text{CuO}_2\text{Cl}_2$ (see Ref. 57). Moreover, the agreement between theory and experiment becomes worse when the two-loop correction has been taken into account.⁶⁰ A possible reason of this inconsistency is the missed contribution from spin diffusion⁶⁰ and the electronic structure of $\text{Sr}_2\text{CuO}_2\text{Cl}_2$ with pockets centered around $(\pi/2, \pi/2)$ as observed by LaRosa *et al.*⁶¹ Thus, for $\text{Sr}_2\text{CuO}_2\text{Cl}_2$ one has to take into account the hoppings between the next nearest and next-next nearest neighbors that are beyond our present consideration.

We now discuss the temperature and doping dependence of plane copper nuclear spin-lattice relaxation rate $^{63}(1/T_1)$. Figure 14 shows the fitted $^{63}(1/T_1)$ to experimental data in lightly doped $\text{La}_{2-x}\text{Sr}_x\text{CuO}_4$. It is seen that the agreement is good for temperatures $T \lesssim J/2$. For temperatures $T > J/2$ the agreement is less satisfactory. This is a bit puzzling but could be due to better account of the ξ values in the low temperature region ($T < J/2$) compared to $T \approx J$ and the preexponential factor $\sim 1/T$ in (24) and in the spin-wave theory,⁷ which is an artifact of the mean-field approach. For carrier free La_2CuO_4 and at $T = 1000$ K ($T \simeq 0.7J$), $\xi \approx 5a$. Obviously, the value of correlation length ξ , as extracted in the limit of large separations¹⁷ satisfies the inequality $\xi^2/a^2 \gg 1$. At temperatures $T < J$ the behavior of $^{63}(1/T_1)$ is smooth: the slope of the curve decreases with increasing T . At high temperatures, $^{63}(1/T_1)$ is expected to have a minimum at $T \approx J$ and to be dominated by spin diffusion at $T \geq J$. The validity of Eq. (24) does not allow to calculate $1/T_1$ at $T > J$. Similar temperature dependence of $^{63}(1/T_1)$ was found in Ref. 19. It was found that the saturation of $^{63}(1/T_1)$ at $T \sim J/2$ is "primarily due to a competition between the spin diffusion over the critical slowing down". The present work shows that the overwhelming contribution arises from strong short-range antiferromagnetic correlations between copper spins and at low temperatures the contribution from spin diffusion to $^{63}(1/T_1)$ is small (see Figure 14).

One may wonder about the results of calculations if we avoid fitting $^{63}(1/T_1)$. Figure 15 shows the results of calculations for $^{63}(1/T_1)$ with fixed decoupling parameter $\zeta = 1$. It is seen, that the theory is able to reproduce the main features of doping and temperature dependence of $^{63}(1/T_1)$, however, in poor agreement with respect to the numerical values.

It is interesting to compare the results of the calculations for carrier free AF system with other theories. After the seminal work,³ Chakravarty and Orbach⁹ predicted the decrease of $^{63}(1/T_1)$ with increasing temperature at low temperatures as $^{63}(1/T_1) \sim T^{3/2} \exp(2\pi\rho_S/k_B T)$. After passing through a wide minimum at $T \sim J/2$ the calculated $^{63}(1/T_1)$ increases with T at high temperatures where the system is recognized to be in the quantum critical (QC) region. On the other hand, using the $1/N$ expansion method on the N -component nonlinear sigma model an apparent formula was obtained for $^{63}(1/T_1)$ in the QC region.⁶ However, the behavior of $^{63}(1/T_1)$ was found to be nearly independent on temperature: $^{63}(1/T_1) \sim (T/J)^{0.028}$. The calculations with thermally excited skyrmions by Belov and Kochelaev⁶² showed that $^{63}(1/T_1)$ has also the nonmonotonic temperature dependence with the slight increase at $T > 0.67J$. In the present theory the calculated value of contribution to $^{63}(1/T_1)$ relaxation rate from spin diffusion at $T = 1000$ K is 550 sec^{-1} in perfect agreement with $300\text{--}600 \text{ sec}^{-1}$ as estimated by Sokol *et al.*⁴⁸ using exact diagonalization technique. However, their estimate was based on the presence of disorder in CuO_2 planes.

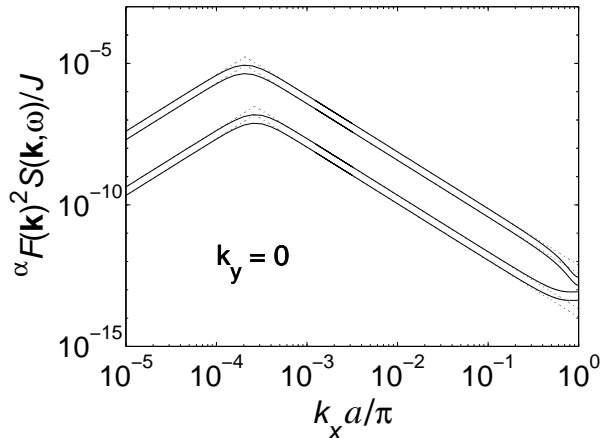


FIG. 11. Log-scale plot of the quantity $\alpha F(\mathbf{k})^2 S(\mathbf{k}, \omega)/J$ versus k_x ($k_y = 0$). The solid lines from down till up: $^{17}F(\mathbf{k})^2 S(\mathbf{k}, \omega_0)/J$ is given for $x = 0.035$ at $T/J = 0.1$ ($T \simeq 140$ K) and $T/J = 0.2$ ($T \simeq 280$ K) with the decoupling parameter $\zeta = 1.3$, $^{63}F(\mathbf{k})^2 S(\mathbf{k}, \omega_c)/J$ is given for carrier free AF ($x = 0$) at $T = 500$ K and $T = 1000$ K with the decoupling parameter $\zeta = 1.8$. The dotted lines are $\alpha F(\mathbf{q}_0)^2 S(\mathbf{q}_0, \omega) k_x^2 / (0.5J\mathbf{q}_0^2)$ for $k_x < \mathbf{q}_0$ and $\alpha F(\mathbf{q}_0)^2 S(\mathbf{q}_0, \omega) \mathbf{q}_0^2 / (0.5Jk_x^2)$ for $k_x > \mathbf{q}_0$.

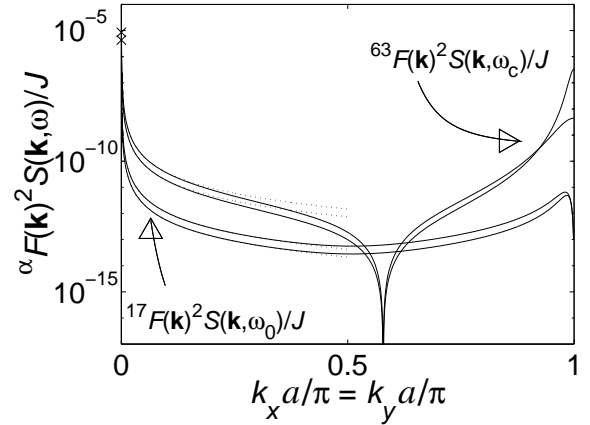


FIG. 12. Semilog-scale plot of the quantity $\alpha F(\mathbf{k})^2 S(\mathbf{k}, \omega)/J$ versus \mathbf{k} along the diagonal of the Brillouin zone ($k_x = k_y$). $^{17}F(\mathbf{k})^2 S(\mathbf{k}, \omega_0)/J$ is given for $x = 0.035$ at $T/J = 0.1$ ($T \simeq 140$ K, lower curve) and $T/J = 0.2$ ($T \simeq 280$ K, upper curve) with the decoupling parameter $\zeta = 1.3$. $^{63}F(\mathbf{k})^2 S(\mathbf{k}, \omega_c)/J$ is given for carrier free AF ($x = 0$) at $T = 500$ K (lower curve at small \mathbf{k}) and $T = 1000$ K (upper curve at small \mathbf{k}) with the decoupling parameter $\zeta = 1.8$. The dotted lines are $\alpha F(\mathbf{q}_0)^2 S(\mathbf{q}_0, \omega) \mathbf{q}_0^2 / (0.5J\mathbf{k}^2)$ for $\mathbf{k} > \mathbf{q}_0$. The lower and upper crosses mark the values of $^{63}F(\mathbf{q}_0)^2 S(\mathbf{q}_0, \omega_c)/J$ at $T = 500$ K and $T = 1000$ K, respectively.

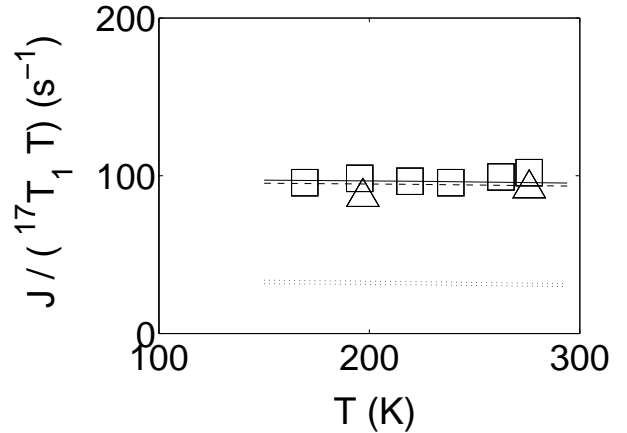


FIG. 13. The calculated temperature and doping dependence of the plane oxygen nuclear spin-lattice relaxation rate $^{17}(1/T_1)$ (lines) and the experimental data for $\text{La}_{2-x}\text{Sr}_x\text{CuO}_4$ as measured by NMR with $x = 0.025$ (triangles) and $x = 0.035$ (squares) from Ref. 57. The experimental points have been rearranged with $J = 1393$ K. The results of calculations with $\omega = 2\pi \times 52$ MHz (9 Tesla) are given for $x = 0.035$ ($\zeta = 1.3$) by solid line and for $x = 0.025$ ($\zeta = 1.6$) by dashed line. The result of calculation with $\omega = 2\pi \times 81.4$ MHz for $x = 0.035$ ($\zeta = 1.3$) coincides with the dashed line. The contribution to $^{17}(1/T_1)$ from the wave vectors in the vicinity of $(\pi/a, \pi/a)$ for $x = 0.035$ with $\zeta = 1$ is shown by upper dotted line and by lower dotted line with $\zeta = 1.3$.

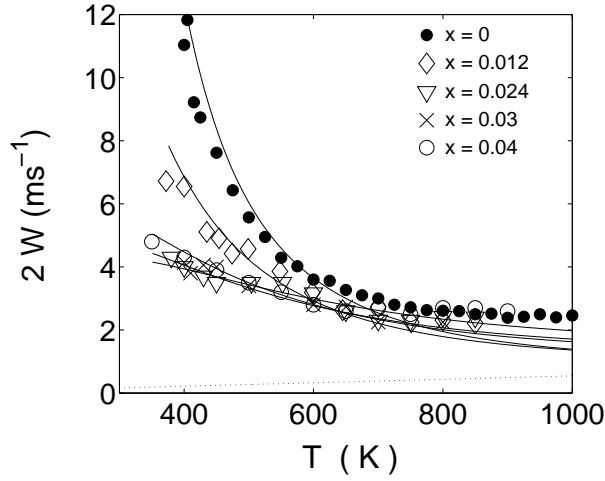


FIG. 14. Temperature and doping dependence of the plane copper nuclear spin-lattice relaxation rate $^{63}(1/T_1) = 2W$ (solid lines) fitted to the experimental data for $\text{La}_{2-x}\text{Sr}_x\text{CuO}_4$ with $x = 0$, $x = 0.012$, $x = 0.024$ and $x = 0.03$ from Ref. 45 and with $x = 0.04$ from Ref. 58. The values of the fitting parameter ζ are shown in the Table 1. The dashed line shows the contribution to $^{63}(1/T_1)$ from spin diffusion for $x = 0$.

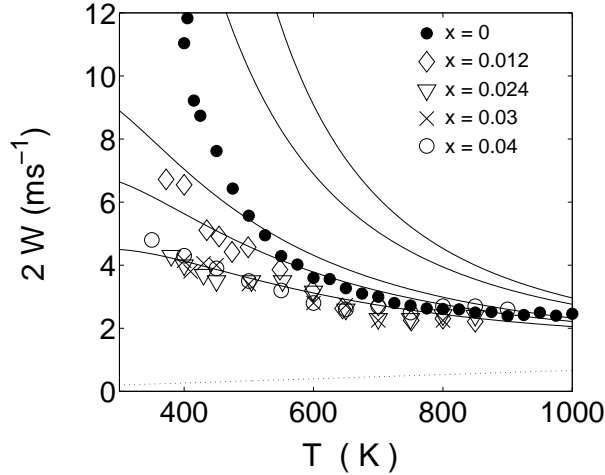


FIG. 15. Recalculated plane copper nuclear spin-lattice relaxation rate $^{63}(1/T_1) = 2W$ with fixed $\zeta = 1$ is shown by solid lines from up till down with increasing doping. The dashed line shows the contribution to $^{63}(1/T_1)$ from spin diffusion for $x = 0.04$ with $\zeta = 1$. The notation is the same as in Fig. 14.

V. CONCLUSION

The theory for relaxation function in the two-dimensional $t - J$ model in the paramagnetic state is presented taking into account the hole subsystem as well as both the electron and antiferromagnetic correlations. The presentation obeys rotational symmetry of the spin correlation functions and is valid for all wave vectors through the Brillouin zone. The fit of effective correlation length ξ_{eff} to experimental data is in agreement with the microsegregation hypothesis, where the effect of doped holes affects the value of correlation length at $T \rightarrow 0$ as, $\xi_0 = 1/nx$, where n is the average distance between the holes along the domain walls. The best fit yields

$n = 1.3$ for samples with $x \lesssim 0.02$ and $n = 2$ for samples with $x > 0.02$. The expression for fourth frequency moment of relaxation shape function is derived within the $t - J$ model. The spin diffusion contribution to relaxation rates is evaluated and is shown to play a significant role in carrier free and doped antiferromagnet in agreement with exact diagonalization calculations. The convergence of contribution from spin diffusion to spin-lattice relaxation rates is preserved by linear response theory and hydrodynamics. At low temperatures the nuclear spin-lattice relaxation rate, $^{63}(1/T_1)$, of plane ^{63}Cu has the main contribution from the AF wavevector (π, π) , and the $^{17}(1/T_1)$, of plane ^{17}O , has the contributions from the wavevectors in the vicinity of (π, π) and small $q \sim 0$. It is shown that the theory is able to explain the main features of experimental data on temperature and doping dependence of copper nuclear spin-lattice relaxation rate in both carrier free La_2CuO_4 and doped $\text{La}_{2-x}\text{Sr}_x\text{CuO}_4$ compounds.

VI. ACKNOWLEDGMENTS

It is a pleasure to thank Dr. A.Yu. Zavidonov for bringing my interest to the present study, Professor M.V. Eremin for discussions, and Professor A. Rigamonti for discussions and hospitality in Pavia University, where part of this work was carried out.

This work was supported in part by INTAS 01-0654 and joint US CRDF - RF Minobr Grant # Y1-P-07-19.

APPENDIX A

Various types of sums over lattice sites utilized for calculation of frequency moments $\langle \omega_{\mathbf{k}}^2 \rangle$ and $\langle \omega_{\mathbf{k}}^4 \rangle$ in the $t - J$ model. The G_{ij} and D_{ij} symbols refer to hopping t and(or) exchange J between the first neighbors, whereas M and Q refer to spin-spin correlation functions c and(or) transfer amplitudes T at the appropriate positions. δ_{ij} is the delta function. The sums for M and Q were calculated for up to $n = |j - i|$ -th neighbors ($n = 2$).

$$\gamma_{\mathbf{k}} \equiv (\cos k_x a + \cos k_y a)/2.$$

$$\frac{1}{N} \sum_{ijlmr} \delta_{im} \delta_{mr} \delta_{lr} D_{rj}^2 G_{rj} M_{rj} e^{i\mathbf{k} \cdot (\mathbf{R}_m - \mathbf{R}_r)} = 4M_1 D^2 G,$$

$$\frac{1}{N} \sum_{ijlmr} \delta_{mr} \delta_{ir} G_{lj} D_{rj}^2 M_{lj} e^{i\mathbf{k} \cdot (\mathbf{R}_m - \mathbf{R}_r)} = 16M_1 D^2 G,$$

$$\frac{1}{N} \sum_{ijlmr} \delta_{ir} G_{lm} G_{mr} G_{rj} M_{lj} M_{mr} e^{i\mathbf{k} \cdot (\mathbf{R}_m - \mathbf{R}_r)} = 36M_1^2 G^3 \gamma_{\mathbf{k}},$$

$$\frac{1}{N} \sum_{ijlmr} \delta_{mr} G_{il} G_{lr} G_{rj} M_{lr} M_{ij} e^{i\mathbf{k} \cdot (\mathbf{R}_m - \mathbf{R}_r)} = 36M_1^2 G^3,$$

$$\frac{1}{N} \sum_{ijlmr} \delta_{mj} G_{il} G_{lm} G_{mr} M_{lm} M_{ir} e^{i\mathbf{k} \cdot (\mathbf{R}_m - \mathbf{R}_r)} = 36M_1^2 G^3 \gamma_{\mathbf{k}},$$

$$\frac{1}{N} \sum_{ijlmr} \delta_{mj} \delta_{lr} \delta_{im} G_{mr}^3 M_{mr} e^{i\mathbf{k} \cdot (\mathbf{R}_m - \mathbf{R}_r)} = 4M_1 G^3 \gamma_{\mathbf{k}},$$

$$\frac{1}{N} \sum_{ijlmr} \delta_{ir} \delta_{lm} D_{mr}^2 G_{rj} M_{rj} e^{i\mathbf{k} \cdot (\mathbf{R}_m - \mathbf{R}_r)} = 16M_1 D^2 G \gamma_{\mathbf{k}},$$

$$\frac{1}{N} \sum_{ijlmr} \delta_{im} \delta_{lm} D_{mj}^2 G_{rj} M_{rj} e^{i\mathbf{k} \cdot (\mathbf{R}_m - \mathbf{R}_r)} = 16M_1 D^2 G \gamma_{\mathbf{k}}^2,$$

$$\frac{1}{N} \sum_{ijlmr} \delta_{ir} \delta_{mr} D_{lr}^2 G_{rj} M_{rj} e^{i\mathbf{k} \cdot (\mathbf{R}_m - \mathbf{R}_r)} = 16M_1 D^2 G,$$

$$\frac{1}{N} \sum_{ijlmr} \delta_{mj} \delta_{il} D_{lm}^2 G_{mr} M_{mr} e^{i\mathbf{k} \cdot (\mathbf{R}_m - \mathbf{R}_r)} = 16M_1 D^2 G \gamma_{\mathbf{k}},$$

$$\frac{1}{N} \sum_{ijlmr} \delta_{ir} G_{lm} G_{mr} G_{rj} M_{rj} M_{lm} e^{i\mathbf{k} \cdot (\mathbf{R}_m - \mathbf{R}_r)} = 64M_1^2 G^3 \gamma_{\mathbf{k}},$$

$$\frac{1}{N} \sum_{ijlmr} \delta_{lr} G_{ir} G_{im} G_{rj} M_{im} M_{rj} e^{i\mathbf{k} \cdot (\mathbf{R}_m - \mathbf{R}_r)} = 64M_1^2 G^3 \gamma_{\mathbf{k}}^2,$$

$$\frac{1}{N} \sum_{ijlmr} \delta_{lj} G_{ij} G_{im} G_{rj} M_{im} M_{rj} e^{i\mathbf{k} \cdot (\mathbf{R}_m - \mathbf{R}_r)} = 64M_1^2 G^3 \gamma_{\mathbf{k}}^3,$$

$$\frac{1}{N} \sum_{ijlmr} \delta_{lj} G_{im} G_{mj} G_{rj} M_{im} M_{rj} e^{i\mathbf{k} \cdot (\mathbf{R}_m - \mathbf{R}_r)} = 64M_1^2 G^3 \gamma_{\mathbf{k}}^2,$$

$$\frac{1}{N} \sum_{ijlmr} \delta_{lj} \delta_{ir} G_{mr} D_{rj}^2 Q_{mj} e^{i\mathbf{k} \cdot (\mathbf{R}_m - \mathbf{R}_r)} = 4D^2 G (3Q_2 + Q_0) \gamma_{\mathbf{k}},$$

$$\frac{1}{N} \sum_{ijlmr} \delta_{mr} \delta_{ij} G_{lj} D_{rj}^2 Q_{lr} e^{i\mathbf{k} \cdot (\mathbf{R}_m - \mathbf{R}_r)} = 4D^2 G (3Q_2 + Q_0),$$

$$\frac{1}{N} \sum_{ijlmr} \delta_{mr} G_{lr} G_{ir} G_{rj} M_{ij} M_{lr} e^{i\mathbf{k} \cdot (\mathbf{R}_m - \mathbf{R}_r)} = 16M_1 G^3 (3M_2 + M_0),$$

$$\frac{1}{N} \sum_{ijlmr} \delta_{ir} G_{lm} G_{mr} G_{rj} M_{mj} M_{lr} e^{i\mathbf{k} \cdot (\mathbf{R}_m - \mathbf{R}_r)} = 4G^3 (3M_2 + M_0)^2 \gamma_{\mathbf{k}},$$

$$\frac{1}{N} \sum_{ijlmr} \delta_{ij} G_{lm} G_{mj} G_{rj} M_{mr} M_{lj} e^{i\mathbf{k} \cdot (\mathbf{R}_m - \mathbf{R}_r)} = 4G^3 (3M_2 + M_0) (M_2 (4\gamma_{\mathbf{k}}^2 - 1) + M_0),$$

$$\begin{aligned} \frac{1}{N} \sum_{ijlmr} \delta_{ij} D_{lj} D_{lm} G_{rj} Q_{mj} M_{lr} e^{i\mathbf{k} \cdot (\mathbf{R}_m - \mathbf{R}_r)} &= 64Q_2 M_2 D^2 G \gamma_{\mathbf{k}}^3 \\ &+ 4 (Q_0 M_0 + 3Q_0 M_2 + 3M_0 Q_2 - 7M_2 Q_2) G^3 \gamma_{\mathbf{k}}, \end{aligned}$$

$$\frac{1}{N} \sum_{ijlmr} \delta_{lj} \delta_{ir} D_{mr} G_{rj} D_{rj} Q_{mj} e^{i\mathbf{k} \cdot (\mathbf{R}_m - \mathbf{R}_r)} = 4D^2 G(3Q_2 + Q_0) \gamma_{\mathbf{k}},$$

$$\frac{1}{N} \sum_{ijlmr} \delta_{lj} G_{ij} G_{mj} G_{rj} M_{im} M_{rj} e^{i\mathbf{k} \cdot (\mathbf{R}_m - \mathbf{R}_r)} = 16M_1 (3M_2 + M_0) G^3 \gamma_{\mathbf{k}}^2,$$

$$\frac{1}{N} \sum_{ijlmr} \delta_{mr} G_{il} G_{lr} G_{rj} M_{ir} M_{lj} e^{i\mathbf{k} \cdot (\mathbf{R}_m - \mathbf{R}_r)} = 4 (3M_2 + M_0)^2 G^3,$$

$$\frac{1}{N} \sum_{ijlmr} \delta_{mj} G_{il} G_{lm} G_{mr} M_{im} M_{lr} e^{i\mathbf{k} \cdot (\mathbf{R}_m - \mathbf{R}_r)} = 4 (3M_2 + M_0)^2 G^3 \gamma_{\mathbf{k}},$$

$$\frac{1}{N} \sum_{ijlmr} \delta_{lr} G_{ir} G_{mr} G_{rj} M_{ir} M_{mj} e^{i\mathbf{k} \cdot (\mathbf{R}_m - \mathbf{R}_r)} = 16M_1 (3M_2 + M_0) G^3 \gamma_{\mathbf{k}},$$

$$\frac{1}{N} \sum_{ijlmr} \delta_{lj} G_{ij} G_{im} G_{rj} M_{ij} M_{mr} e^{i\mathbf{k} \cdot (\mathbf{R}_m - \mathbf{R}_r)} = 36M_1^2 G^3 \gamma_{\mathbf{k}},$$

$$\frac{1}{N} \sum_{ijlmr} \delta_{mj} G_{lm} G_{im} G_{mr} M_{ir} M_{lm} e^{i\mathbf{k} \cdot (\mathbf{R}_m - \mathbf{R}_r)} = 16M_1 G^3 (3M_2 + M_0) \gamma_{\mathbf{k}},$$

$$\frac{1}{N} \sum_{ijlmr} \delta_{lr} G_{ir} G_{im} G_{rj} M_{ir} M_{mj} e^{i\mathbf{k} \cdot (\mathbf{R}_m - \mathbf{R}_r)} = M_1^2 G^3 (12 + 16\gamma_{\mathbf{k}}^2 + 8 \cos k_x a \cos k_y a),$$

$$\frac{1}{N} \sum_{ijlmr} \delta_{ij} G_{lm} G_{mj} G_{rj} M_{lr} M_{mj} e^{i\mathbf{k} \cdot (\mathbf{R}_m - \mathbf{R}_r)} = M_1^2 G^3 (12 + 16\gamma_{\mathbf{k}}^2 + 8 \cos k_x a \cos k_y a),$$

$$\frac{1}{N} \sum_{ijlmr} \delta_{lj} G_{ij} G_{mj} G_{rj} M_{ij} M_{mr} e^{i\mathbf{k} \cdot (\mathbf{R}_m - \mathbf{R}_r)} = 16M_1 G^3 (M_2 (4\gamma_{\mathbf{k}}^2 - 1) + M_0),$$

$$\frac{1}{N} \sum_{ijlmr} \delta_{lj} G_{ij} G_{im} G_{rj} M_{mj} M_{ir} e^{i\mathbf{k} \cdot (\mathbf{R}_m - \mathbf{R}_r)} = 64M_2^2 G^3 \gamma_{\mathbf{k}}^3 + 4 (M_0^2 + 6M_0 M_2 - 7M_2^2) G^3 \gamma_{\mathbf{k}},$$

$$\frac{1}{N} \sum_{ijlmr} \delta_{mj} G_{lm} G_{im} G_{mr} M_{il} M_{mr} e^{i\mathbf{k} \cdot (\mathbf{R}_m - \mathbf{R}_r)} = 16M_1 (3M_2 + M_0) G^3 \gamma_{\mathbf{k}},$$

$$\frac{1}{N} \sum_{ijlmr} \delta_{ir} G_{lr} G_{mr} G_{rj} M_{lm} M_{rj} e^{i\mathbf{k} \cdot (\mathbf{R}_m - \mathbf{R}_r)} = 16M_1 (3M_2 + M_0) G^3 \gamma_{\mathbf{k}},$$

$$\frac{1}{N} \sum_{ijlmr} \delta_{lr} \delta_{ij} D_{mj} G_{rj} D_{rj} Q_{mr} e^{i\mathbf{k} \cdot (\mathbf{R}_m - \mathbf{R}_r)} = 4D^2 G(Q_2(4\gamma_{\mathbf{k}}^2 - 1) + Q_0),$$

APPENDIX B

In this appendix the relations to compare the result for frequency moments of $F(\mathbf{k}, \omega)$ in carrier free 2DHAF are given.

For the second and fourth moments the result was¹⁶

$$\langle \omega_{\mathbf{k}}^2 \rangle_{2\text{DHAF}} = -\frac{8J(1-\gamma_{\mathbf{k}})}{\chi(\mathbf{k})N} \sum_{\mathbf{q}} \gamma_{\mathbf{q}} S(\mathbf{q}), \quad (85)$$

and

$$\langle \omega_{\mathbf{k}}^4 \rangle_{2\text{DHAF}} = -\frac{128J^3}{\chi(\mathbf{k})N^2} \sum_{\mathbf{p}, \mathbf{q}} S(\mathbf{p}) S(\mathbf{q}) F(\mathbf{k}, \mathbf{p}, \mathbf{q}), \quad (86)$$

where

$$\begin{aligned} F(\mathbf{k}, \mathbf{p}, \mathbf{q}) \simeq & \gamma_{\mathbf{k}} (-2\gamma_{\mathbf{p}}\gamma_{\mathbf{q}} - 10\gamma_{\mathbf{p}}\gamma_{\mathbf{q}}^2 - 4\gamma_{\mathbf{p}}\gamma_{\mathbf{q}}^3 + \gamma_{\mathbf{p}}^2\gamma_{\mathbf{q}}^2) \\ & + \gamma_{\mathbf{k}}^2 (4\gamma_{\mathbf{p}}\gamma_{\mathbf{q}} + 3\gamma_{\mathbf{p}}\gamma_{\mathbf{q}}^2) - 2\gamma_{\mathbf{k}}^3\gamma_{\mathbf{p}}\gamma_{\mathbf{q}} + 5\gamma_{\mathbf{p}}\gamma_{\mathbf{q}}^2 \\ & - \gamma_{\mathbf{p}}^2\gamma_{\mathbf{q}}^2 + \gamma_{\mathbf{p}}\gamma_{\mathbf{q}}^3 + 5\gamma_{\mathbf{p}}\gamma_{\mathbf{q}}\gamma_{\mathbf{k}-\mathbf{q}}^2 + \gamma_{\mathbf{k}+\mathbf{p}}^2\gamma_{\mathbf{q}}^2 \\ & + 2\gamma_{\mathbf{p}}\gamma_{\mathbf{k}-\mathbf{q}}^2 - 2\gamma_{\mathbf{p}}\gamma_{\mathbf{k}-\mathbf{q}}^3 - \gamma_{\mathbf{k}+\mathbf{p}}\gamma_{\mathbf{k}-\mathbf{q}}\gamma_{\mathbf{k}+\mathbf{p}-\mathbf{q}}. \end{aligned} \quad (87)$$

Using the relation between correlation functions in momentum and site representation:

$$\begin{aligned} S(\mathbf{k}) \equiv \langle S_{\mathbf{k}}^z S_{-\mathbf{k}}^z \rangle &= \sum_{|i-j| \leq 2} \langle S_i^z S_j^z \rangle e^{i\mathbf{k} \cdot (\mathbf{R}_i - \mathbf{R}_j)} = \\ &= c_0 + 4c_1\gamma_{\mathbf{k}} + 4c_2(4\gamma_{\mathbf{k}}^2 - \cos k_x a \cos k_y a - 1), \end{aligned} \quad (88)$$

performing the summation over \mathbf{k} and \mathbf{q} in (86) and using the necessary types of integrals (sums) over the Brillouin zone as given below, we obtain the same expression, as shown in (68), with $t_{\text{eff}} = 0$ and settling to unity the decoupling parameter $\zeta = 1$. The integrals (sums) were calculated analytically and checked numerically.

$$\gamma_{\mathbf{q}} \equiv (\cos q_x a + \cos q_y a)/2.$$

$$\sum_{\mathbf{p}} \gamma_{\mathbf{p}}^4 = \frac{9}{64}, \quad \sum_{\mathbf{p}} \gamma_{\mathbf{p}}^2 = \frac{1}{4}, \quad \sum_{\mathbf{q}} \gamma_{\mathbf{k}-\mathbf{q}}^2 = \frac{1}{4},$$

$$\sum_{\mathbf{p}, \mathbf{q}} \cos p_x a \cos p_y a \gamma_{\mathbf{k}+\mathbf{p}} \gamma_{\mathbf{k}-\mathbf{q}} \gamma_{\mathbf{k}+\mathbf{p}-\mathbf{q}} = \frac{1}{32} \gamma_{\mathbf{k}},$$

$$\sum_{\mathbf{p}, \mathbf{q}} \gamma_{\mathbf{p}}^2 \gamma_{\mathbf{q}}^2 \gamma_{\mathbf{k}+\mathbf{p}} \gamma_{\mathbf{k}-\mathbf{q}} \gamma_{\mathbf{k}+\mathbf{p}-\mathbf{q}} = \frac{1}{256} \left(\gamma_{\mathbf{k}}^3 + \frac{5}{4} \gamma_{\mathbf{k}} \cos k_x a \cos k_y a + \frac{45}{16} \gamma_{\mathbf{k}} \right),$$

$$\sum_{\mathbf{p}, \mathbf{q}} \cos p_x a \cos p_y a \gamma_{\mathbf{k}+\mathbf{p}}^2 \gamma_{\mathbf{k}-\mathbf{q}} \gamma_{\mathbf{k}+\mathbf{p}-\mathbf{q}} = \frac{3\gamma_{\mathbf{k}}}{512} (2 \cos k_x a \cos k_y a + 1),$$

$$\sum_{\mathbf{p}, \mathbf{q}} \cos p_x a \cos p_y a \cos q_x a \cos q_y a \gamma_{\mathbf{k}+\mathbf{p}} \gamma_{\mathbf{k}-\mathbf{q}} \gamma_{\mathbf{k}+\mathbf{p}-\mathbf{q}} = \frac{1}{64} \cos k_x a \cos k_y a \gamma_{\mathbf{k}},$$

$$\sum_{\mathbf{p}} \gamma_{\mathbf{p}} = 0, \quad \sum_{\mathbf{q}} \gamma_{\mathbf{q}} \gamma_{\mathbf{k}-\mathbf{q}}^2 = 0, \quad \sum_{\mathbf{p}} \gamma_{\mathbf{p}}^3 = 0,$$

$$\sum_{\mathbf{p}} \gamma_{\mathbf{p}} \cos p_x a \cos p_y a = 0, \quad \sum_{\mathbf{q}} \gamma_{\mathbf{q}}^3 \gamma_{\mathbf{k}-\mathbf{q}}^2 = 0,$$

$$\sum_{\mathbf{q}} \gamma_{\mathbf{q}}^2 \gamma_{\mathbf{k}-\mathbf{q}}^2 = \frac{1}{16} \left(\frac{3}{4} + \frac{1}{2} \cos k_x a \cos k_y a + \gamma_{\mathbf{k}}^2 \right),$$

$$\sum_{\mathbf{q}} \gamma_{\mathbf{q}} \gamma_{\mathbf{k}-\mathbf{q}}^3 = \frac{9}{64} \gamma_{\mathbf{k}}, \quad \sum_{\mathbf{q}} \gamma_{\mathbf{q}}^2 \cos q_x a \cos q_y a = \frac{1}{8},$$

$$\sum_{\mathbf{q}} \gamma_{\mathbf{k}-\mathbf{q}}^2 \cos q_x a \cos q_y a = \frac{1}{8} \cos k_x a \cos k_y a,$$

$$\sum_{\mathbf{p}, \mathbf{q}} \gamma_{\mathbf{k}+\mathbf{p}} \gamma_{\mathbf{k}-\mathbf{q}} \gamma_{\mathbf{k}+\mathbf{p}-\mathbf{q}} = \frac{1}{16} \gamma_{\mathbf{k}},$$

$$\sum_{\mathbf{p}, \mathbf{q}} \gamma_{\mathbf{p}}^2 \gamma_{\mathbf{k}+\mathbf{p}} \gamma_{\mathbf{k}-\mathbf{q}} \gamma_{\mathbf{k}+\mathbf{p}-\mathbf{q}} = \frac{9}{256} \gamma_{\mathbf{k}},$$

* e-mail: *iL* @ ksu.ru

- ¹ A. Rigamonti, F. Borsa, and P. Carretta, Rep. Prog. Phys. **61**, 1367 (1998).
- ² E. Dagotto, Rev. Mod. Phys. **66**, 763 (1994).
- ³ S. Chakravarty, B.I. Halperin, and D.R. Nelson, Phys. Rev. Lett. **60**, 1057 (1988); Phys. Rev. B **39**, 2344 (1989).
- ⁴ Y. Endoh, K. Yamada, R.J. Birgeneau, D.R. Gabbe, H.P. Jenssen, M.A. Kastner, C.J. Peters, P.J. Picone, T.R. Thurston, J.M. Tranquada, G. Shirane, Y. Hidaka, M. Oda, Y. Enomoto, M. Suzuki, and T. Murakami, Phys. Rev. B **37**, 7443 (1988).
- ⁵ P. Hasenfratz and F. Niedermayer, Phys. Lett. B **268**, 231 (1991); Z. Phys. B **92**, 91 (1993).
- ⁶ A.V. Chubukov, S. Sachdev, and J. Ye, Phys. Rev. B **49**, 11 919 (1994); A.V. Chubukov and S. Sachdev, Phys. Rev. Lett. **71**, 169 (1993).
- ⁷ A. Sokol, R.R.P. Singh, and N. Elstner, Phys. Rev. Lett. **76**, 4416 (1996).
- ⁸ S.I. Belov and B.I. Kochelaev, Solid State Commun. **103**, 249 (1997).
- ⁹ S. Chakravarty and R. Orbach, Phys. Rev. Lett. **64**, 224 (1990).
- ¹⁰ S. Chakravarty, in *High-Temperature Superconductivity*, Proceedings of the Los Alamos Symposium edited by K.S. Bedell, D. Coffey, D.E. Meltzer, D. Pines, and J.R. Schrieffer (Addison-Wesley, Redwood City, CA, 1990).
- ¹¹ A.J. Millis, H. Monien, and D. Pines, Phys. Rev. B **42**, 167 (1990).
- ¹² A.V. Chubukov, D. Pines, and J. Schmalian, in "The Physics of Conventional and Unconventional Superconductors", eds. by K.H. Bennemann and J.B. Ketterson, Vol. 1 (Springer-Verlag, 2003) (review).
- ¹³ P.W. Anderson, Science **235**, 1196 (1987).
- ¹⁴ H. Mori, Prog. Theor. Phys. **33**, 423 (1965); **34**, 399 (1965).
- ¹⁵ R. Zwanzig, Phys. Rev. **124**, 983 (1961); R. Zwanzig, K.S.J. Nordholm, and W.C. Mitchell, Phys. Rev. A **5**, 2680 (1972).
- ¹⁶ S.W. Lovesey and R.A. Meserve, J. Phys. C **6**, 79 (1973).
- ¹⁷ A.Yu. Zavidonov and D. Brinkmann, Phys. Rev. B **58**, 12 486 (1998).
- ¹⁸ H. Mori and K. Kawasaki, Prog. Theor. Phys. **27**, 529 (1962).
- ¹⁹ Y.-J. Wang, M.-R. Li, and C.-D. Gong, Phys. Rev. B **56**, 10 982 (1997).
- ²⁰ T. Moriya, J. Phys. Soc. Jpn. **18**, 516 (1963); *Spin Fluctuations in Itinerant Electron Magnetism* (Springer, Berlin, 1985); see also T. Moriya, Prog. Theor. Phys. **16**, 641 (1956); P.W. Anderson and P.R. Weiss, Rev. Mod. Phys. **25**, 269 (1953).
- ²¹ A. Yu. Zavidonov, I.A. Larionov and D. Brinkmann, Phys. Rev. B **61**, 15 462 (2000).
- ²² A. Yu. Zavidonov and D. Brinkmann, Phys. Rev. B **63**, 132506 (2001).
- ²³ D.G. McFadden and R.A. Tahir-Kheli, Phys. Rev. B **1**, 3649 (1970); *ibid.* **1**, 3671 (1970).
- ²⁴ A.P. Young and B.S. Shastry, J. Phys. C **15**, 4547 (1982).
- ²⁵ J. Kondo and K. Yamaji, Prog. Theor. Phys. **47**, 807 (1972).
- ²⁶ B. Keimer, N. Belk, R.J. Birgeneau, A. Cassanho, C.Y. Chen, M. Greven, M.A. Kastner, A. Aharony, Y. Endoh, R.W. Erwin, and G. Shirane, Phys. Rev. B **46**, 14 034 (1992).
- ²⁷ N.M. Plakida, R. Hayn, and J.-L. Richard, Phys. Rev. B **51**, 16 599 (1995).
- ²⁸ G. Baskaran, Z. Zou, and P.W. Anderson, Solid State Commun. **63**, 973 (1987).
- ²⁹ F.C. Zhang and T.M. Rice, Phys. Rev. B **37**, 3759 (1988).
- ³⁰ M.V. Eremin, R. Markendorf and S.V. Varlamov, Solid State Commun. **88**, 15 (1993); M.V. Eremin, S.G. Solovjanov, S.V. Varlamov, D. Brinkmann, M. Mali, R. Markendorf, and J. Roos, Pis'ma Zh. Eksp. i Teor. Fiz. **60**, 118 (1994) [JETP Lett. **60**, 125 (1994)]; M.V. Eremin, S.G. Solovjanov, S.V. Varlamov, Zh. Eksp. i Teor. Fiz. **112**, 1763 (1997) [JETP **85**, 963 (1997)].
- ³¹ A.A. Abrikosov, J.C. Campuzano, and K. Gofron, Physica (Amsterdam) **C 214**, 73 (1993).
- ³² L.M. Roth, Phys. Rev. **184**, 451 (1969).
- ³³ P. Unger and P. Fulde, Phys. Rev. B **48**, 16 607 (1993).
- ³⁴ B. Mehlh, H. Eskes, R. Hayn, and M.B.J. Meinders, Phys. Rev. B **52**, 2463 (1995).
- ³⁵ S.P. Bowen, J. Math. Phys. **16**, 620 (1975).
- ³⁶ A.B. Harris and R.V. Lange, Phys. Rev. **157**, 295 (1967).
- ³⁷ I. Eremin, M. Eremin, S. Varlamov, D. Brinkmann, M. Mali, and J. Roos, Phys. Rev. B **56**, 11 305 (1997).
- ³⁸ J. Beenen and D.M. Edwards, Phys. Rev. B **52**, 13 636 (1995).
- ³⁹ J. Hubbard and K.P. Jain, J. Phys. C (Proc. Roy. Phys. Soc.) **1**, 1650 (1968).
- ⁴⁰ R.J. Birgeneau, D.R. Gabbe, H.P. Jenssen, M.A. Kastner, P.J. Picone, T.R. Thurston, G. Shirane, Y. Endoh, M. Sato, K. Yamada, Y. Hidaka, M. Oda, Y. Enomoto, M. Suzuki, and T. Murakami, Phys. Rev. B **38**, 6614 (1988).
- ⁴¹ F. Borsa, P. Carreta, J.H. Cho, F.C. Chou, Q. Hu, D.C. Johnston, A. Lascialfari, D.R. Torgeson, R.J. Gooding, N.M. Salem, and K.J.E. Vos, Phys. Rev. B **52**, 7334 (1995).
- ⁴² J.M. Tranquada, B.J. Sternlieb, J.D. Axe, Y. Nakamura, and S. Uchida, Nature **375**, 561 (1995); J.M. Tranquada, J.D. Axe, N. Ichikawa, Y. Nakamura, S. Uchida, and B. Nachumi, Phys. Rev. B **54**, 7489 (1996); J.M. Tranquada, J.D. Axe, N. Ichikawa, A.R. Moodenbaugh, Y. Nakamura, and S. Uchida, Phys. Rev. Lett. **78**, 338 (1997); J.M. Tranquada, in *Neutron Scattering in Layered Copper-Oxide Superconductors*, ed. A. Furrer (Kluwer, Dordrecht, 1998), p. 225.
- ⁴³ P. Carretta, A. Rigamonti, and R. Sala, Phys. Rev. B **55**, 3734 (1995).
- ⁴⁴ R.J. Birgeneau, M. Greven, M.A. Kastner, Y.S. Lee, B.O. Wells, Y. Endoh, K. Yamada, and G. Shirane, Phys. Rev. B **59**, 13 788 (1999).
- ⁴⁵ P. Carretta, F. Tedoldi, A. Rigamonti, F. Galli, F. Borsa, J.H. Cho and D.C. Johnston, Eur. Phys. J. B **10**, 233 (1999).
- ⁴⁶ P.G. de Gennes, J. Phys. Chem. Solids **4**, 223 (1958); H.S. Bennett and P.C. Martin, Phys. Rev. **138**, A608 (1965).
- ⁴⁷ T. Morita, Phys. Rev. B **6**, 3385 (1972).
- ⁴⁸ A. Sokol, E. Gagliano, and S. Bacci, Phys. Rev. B **47**, 14 646 (1993).
- ⁴⁹ M.F. Collins, Phys. Rev. B **4**, 1588 (1971).
- ⁵⁰ J. Bonca and J. Jaklic, Phys. Rev. B **51**, 16 083 (1995).
- ⁵¹ M. Makivić and M. Jarrell, Phys. Rev. Lett. **68**, 1770 (1992).
- ⁵² Dieter Forster, *Hydrodynamic Fluctuations, Broken Symmetry, and Correlation Functions*, Frontiers in Physics,

- Vol. **47** (Benjamin, Reading, MA, 1975); see also P. Kopietz, Phys. Rev. B **57**, 7829 (1998).
- ⁵³ F. Mila and T.M. Rice, Physica C **157**, 561 (1989).
- ⁵⁴ B.S. Shastry, Phys. Rev. Lett. **63**, 1288 (1989).
- ⁵⁵ Y. Zha, V. Barzykin, and D. Pines, Phys. Rev. B **54**, 7561 (1996).
- ⁵⁶ H. Monien, D. Pines, and M. Takigawa, Phys. Rev. B **43**, 258 (1991); H. Monien, P. Monthoux, and D. Pines, *ibid.* **43**, 275 (1991).
- ⁵⁷ K.R. Thurber, A.W. Hunt, T. Imai, F.C. Chou, and Y.S. Lee, Phys. Rev. Lett. **79**, 171 (1997).
- ⁵⁸ T. Imai, C.P. Slichter, K. Yoshimura, and K. Kosuge, Phys. Rev. Lett. **70**, 1002 (1993).
- ⁵⁹ S. Chakravarty, M.P. Gelfand, P. Kopietz, R. Orbach, and M. Wollensak, Phys. Rev. B **43**, 2796 (1991).
- ⁶⁰ P. Kopietz and S. Chakravarty, Phys. Rev. B **56**, 3338 (1997).
- ⁶¹ S. LaRosa, I. Vobornik, F. Zwick, H. Berger, M. Grioni, G. Margaritondo, R.J. Kelley, M. Onellion, and A. Chubukov, Phys. Rev. B **56**, R525 (1997).
- ⁶² S.I. Belov and B.I. Kochelaev, Solid State Commun. **106**, 207 (1998).